Effects of Inlet Design on Hydraulic Efficiency and Sediment Cleanout of Bridge Deck Drains

By
Alexander T. Michalek
B.S., University of Kansas, 2018

Submitted to the graduate degree program in Civil, Environmental, and Architectural Engineering and the Graduate Faculty of the University of Kansas in partial fulfillment of the requirements for the degree of Master of Science.

_____

Chair: Admin Husic, Ph.D.

_____

Joshua Roundy, Ph.D.

_____

Amy Hansen, Ph.D.

_____

C. Bryan Young, Ph.D.

Date Defended: 23 April 2021

The thesis committee for Alexander T. Michalek certifies that this is the approved version of the following thesis:

Effects of Inlet Design on Hydraulic Efficiency and Sediment Cleanout of Bridge Deck Drains

Chair: Admin Husic, Ph.D.

Joshua Roundy, Ph.D.

Amy Hansen, Ph.D.

C. Bryan Young, Ph.D.

Date Approved: 28 April 2021

Abstract

Bridge deck drainage is driven by the hydraulic efficiency of inlets, which can be affected by grate design, downspout configuration, and debris accumulation. Inadequate drainage can result in hydroplaning, which can diminish highway safety. To evaluate the controls on drainage inlet efficiency and compare currently deployed inlet design performances, 576 controlled laboratory experiments were conducted testing grate type (rectangular bar vs curved vane) and downspout configuration (square vs circular and 20 cm vs 25 cm) across a range of flow rates, cross slopes, and longitudinal slopes. Experimental results found no significant difference for hydraulic efficiency across grate design and flow rates but suggest that the design equations may not accurately estimate inlet hydraulic efficiencies due to unaccounted splashover behavior observed in grates. An additional 144 sediment transport experiments showed that curved vane grates had better debris removal than bar grates under most flow conditions. These results can be used with hydroclimatological data to improve location-specific grate design selection and reduce debris susceptibility, maintenance costs, and the risk of hydroplaning.

Acknowledgements

I would like to thank Mike Orth and the Kansas Department of Transportation for providing funding for this project and my Master of Science. This opportunity allowed me to explore classes and research to find my interests in the field of water resource engineering. I want to thank my advisor, Dr. Admin Husic, for his guidance throughout my graduate studies. His commitment to research helped to develop my work ethic and I am grateful for the multiple research projects I was able to work with him on during my Master's. I am thankful to Dr. Joshua Roundy for selecting me for this project and being an outstanding professor. The concepts for hydrology, statistics, and water resource engineering I learned during my undergraduate and graduate studies with him helped me to discover my interest in the field of hydraulics and hydrology. I also would like to thank Dr. Amy Hansen for her advice throughout this project on experimental design and execution. Finally, I would like to thank Dr. C. Bryan Young for being an additional member on my committee.

The last six years I have spent as an undergraduate and graduate student in the CEAE department at the University of Kansas have been some of the most memorable of my life and I am grateful for all the professors that have helped me throughout my time. I have also met many great students along the way who have helped aid in my understanding of concepts. I am especially grateful for meeting my colleague and dear friend, Amirreza Zarnaghsh, who during my graduate study was always available and willing to help with research, discuss course work, and take study breaks playing tennis.

Table of Contents

[1]Chapters are adapted from a manuscript under review. The author of the thesis is the first author with co-authors Dr. Admin Husic, Dr. Joshua Roundy, and Dr. Amy Hansen.

List of Figures

List of Tables

Chapter 1: Introduction

Bridge deck drainage is necessary for removing stormwater runoff as deck ponding increases the potential for hydroplaning, which can cause loss of vehicle control and human life (Qian et al. 2015). Deck drainage inlet designs typically consist of a grate, inlet pan, and downspout. Inlet spacing requirements are governed by hydraulic efficiency equations given in Hydraulic Engineering Circular 21 (HEC-21) (Young et al., 1993). Drainage inlets are often plagued by debris accumulation which reduces their ability to convey runoff from the roadway (Gómez et al. 2019). Currently, roadway drainage literature primarily focuses on the drainage hydraulic efficiency (Johnson and Chang 1984; Holley et al. 1992; Young et al. 1993; Hammonds and Holley 1995; McEnroe et al. 1999; Qian et al., 2016; Schalla et al. 2017; Muhammad 2018; Li et al. 2019) with none examining the impact of grate design on accumulated debris removal.

Bridge decks commonly have a constant cross slope to convey runoff to the outer curb where it accumulates as gutter flow. Gutter flow can be characterized by a modified Manning's equation (Izzard 1946, 1950) expressed as:

$$Q=(\frac{k_g}{n})S_x^{1.67}S^{0.5}T^{2.67} \quad (1)$$

Where Q = total gutter flow rate, k_g = 0.375 for SI units, n = Manning's roughness coefficient, T = width of flow, S_x = cross slope, and S = longitudinal slope. Bridge deck drainage is typically designed such that gutter flow does not extend into the roadway by constraining T in the analysis. Hydraulic efficiency (E) of grated inlets is determined by the ratio of intercepted flow to total gutter flow and can be estimated for various grate types (Johnson and Chang 1984) as:

$$E=\frac{Q_c}{Q}=R_fE_o+R_s(1-E_o) \quad (2)$$

Where Q_c = intercepted flow, R_f = fraction of frontal flow entering the inlet, R_s = fraction of side flow entering the inlet, E_o = ratio of frontal inlet flow to total gutter flow, and E = overall efficiency. The non-adjusted, standard theoretical E_o relationship (Johnson and Chang 1984) is defined as:

$$E_o = 1-(1- \frac{W}{T})^{8/3} \quad (3)$$

Where W = the opening width of the inlet. Frontal and side flow ratios are given as (Young et. al. 1996):

$$R_f=1-0.3(v-v_o) \quad (4)$$

$$R_s = \frac{1}{\left[1+\frac{0.15v^{1.8}}{0.55S_xL_g^{2.3}}\right]} \quad (5)$$

Where v = velocity of flow in the gutter, v_o = grate specific splashover velocity, and L_g = the length of the inlet parallel to the flow as shown in Figure 1. An assessment of the accuracy of standard design equations is important as they do not explicitly incorporate inlet pan or downspout design and grate-specific values are generalized. Inaccurate design could lead to safety concerns or unnecessary costs if the number of inlets are underestimated or overestimated, respectively.

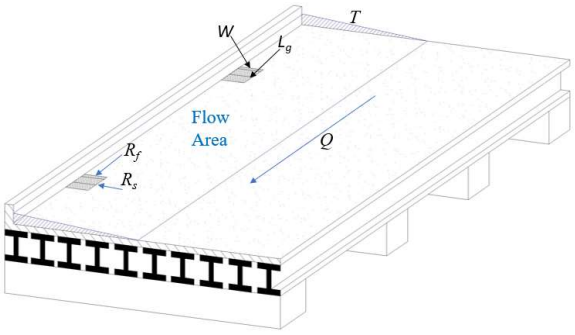

Figure 1. Conceptual Diagram of a bridge deck with drainage inlets depicting terms of Q, Rf, Rs, and T.

To understand issues impacting bridge deck drainage in the USA, state departments of transportation (DOTs) were surveyed and found that 21 out of 22 responses reported issues with

inlet clogging (see Appendix A for more information). Survey results support the need for further research and analysis of the impact of grate design on debris removal. First, debris in inlets limits efficiency of inlets as capture areas decreases which can adversely affect motorist safety. Second, if inlet clogging is common, it can be costly to implement routine preventative maintenance. Additionally, clogged inlets will remove less runoff which may deteriorate primary traffic lanes as corrosive aqueous substances may pond for longer, incurring additional costs to repair structural damages (Bakr et al. 2020). However, because precipitation patterns and intensities vary considerably across the United States, state-specific DOT designs may need to vary accordingly. Thus, experimentation is needed to understand how inlet design can be informed by local precipitation regimes to optimize sediment cleanout.

In this study, curved vane and rectangular bar grated inlets were examined to improve the characterization of hydraulic efficiency and sediment cleanout for a range of current bridge deck drainage inlet designs. To achieve this goal, two specific objectives were identified. The first objective was to quantify uncertainties in hydraulic efficiency between various combinations of downspout size, downspout shape, and grate type by comparing the measured efficiency with the theoretical efficiency given by standard design. The second objective was to quantify the potential of debris removal between two grate types under varying precipitation regimes and assess the implications to design.

Chapter 2: Methods

Appendix B contains a literature review regarding related studies discussing their methods and analysis used as a guide for the experiments.

Hydraulic Efficiency

The experiments were conducted in a 1:9 scale laboratory model, representing a 6.4-m single lane highway and shoulder on a bridge deck (Figure 2a). The model was suspended in a 10.16-m-long, 0.91-m-wide, and 1.52-m-deep flume with cables attached to supports across the top of the flume. The width of the model was 0.71-m with a length of 10.16-m and the cable supports allowed for full adjustability of longitudinal slope, S, and cross slope, S_x, across the range of 0.5 to 4% and 2 to 6%, respectively.

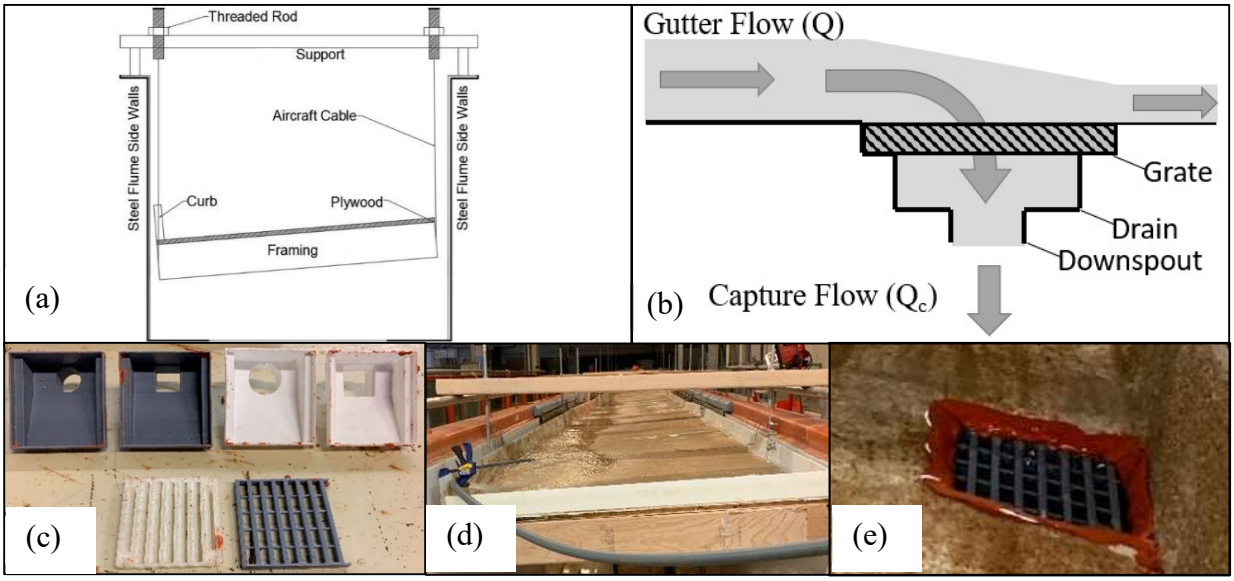

Figure 2. (a) Cross-sectional and (b) side profile views of experimental bridge deck set-up with dimensions, layout, and materials used. Images of (c) 3-D printed inlet and grate designs, (d) above-deck inflow set-up, and (e) placement of inlet on the surface.

Four openings in the deck gutter were created to insert and interchange grate inlet designs (Figure 2b). The inlets and grates were scaled using a modeling software and 3-D printed for greater precision and control of design (Figure 2c). The four inlet types printed for this study all

simulated 0.61-m square openings. Square and circular downspout shapes were tested for two widths/diameters (20-cm and 25-cm). Bar and vane grates were all scaled and printed following design drawings provided by Kansas (KDOT) and Illinois (ILDOT) Departments of Transportation, respectively (Appendix G). The one state DOT that did not report issues related to inlet clogging was the only one to use curved vane grates rather than rectangular bar grates, providing some qualitative basis for a comparison of the two grate types. Upstream inflow to the model was provided by a hose with a calibrated flow meter (Tuthill TT10PN) (Figure 2d). The hose was placed against the curb of the deck facing downslope to immediately simulate channelized gutter flow. Measurement tapes were attached 0.76-m upstream of each inlet to measure the spread of water. To represent the roughness of bridge deck surfaces, the standard Manning's n used by KDOT (0.016) was scaled accordingly to 0.012 by application of a length ratio relationship and converted to a sand grain equivalent (0.5 mm silica) that was adhered to the deck (Appendix C.1).

The first set of experiments were conducted to quantify the uncertainty in hydraulic efficiency, *E,* and assess differences based on downspout configuration and grate type. Flow rate and spread were recorded at four evenly spaced inlets across a range of inflows (Figure 2e). Flow captured by each inlet was measured using containers placed under the deck. To calculate captured flow, collected water was weighed and divided by experiment runtime and water density. The system was automated with solenoid valves to drain the collection bins between experiments. The procedure for this part of the study was to run the experimental series listed in Table 1 at low (0.68 m^3/h), medium (1.02 m^3/h), and high (1.59 m^3/h) inflow regimes with three replicates per configuration. For each trial, the deck surface was wetted by inflow for 30 seconds prior to data

collection to remove the influence of surface material on water spread. Each experimental run lasted three minutes allowing for starting and ending captured weights and spreads to be recorded.

Table 1.Hydraulic efficiency experimental testing conditions.

Component	Number of Iterations	Iteration Types
Cross Slope	2	2%, 6%
Longitudinal Slope	4	0.5%, 1%, 2%, 4%
Inflow	3	0.68 m^3/h, 1.02 m^3/h, 1.59 m^3/h
Downspout shape	2	Circular, Square
Downspout Size	2	20 cm, 25 cm
Grate Type	2	Bar, Vane
Replicates	3	-
Number of Trials	576	

Captured flow was converted to efficiency using the gutter flow between inlets determined by the known inflow rate. Spread was converted to a dimensionless width-to-spread ratio, *WT*, for analysis with the efficiency relationship provided by Eqn. 3. The grate-specific splashover velocity for the bar and vane grate were set as 1.4 m/s and 1.8 m/s, respectively, as determined from design charts in Johnson and Chang (1984). The total uncertainty (U) was defined as the residual between the theoretical efficiency and experimentally observed efficiency. Further, U can be subdivided into two components, experimental uncertainty (U_e) and hydraulic uncertainty (U_h) and is given by the following equation:

$$U = U_e + U_h \tag{6}$$

Within this framework, U_e is the experimental uncertainty that results from inconsistencies due to small variations in conditions related to the physical experiment, while U_h is a result of consistent deviations between the experiment and theoretical efficiencies that indicate a hydraulically inconsistent relationship. To quantify these uncertainties the width-to-spread ratio is broken up into bins of 0.1 and U_h is calculated as the mean uncertainty (U) within the bin and U_e is calculated as the standard deviation of uncertainty (U) in each bin. This approach breaks up the total

uncertainty into consistent deviations between the experiments and the design equation (U_h) that can be tested for statistical significance using the non-parametric Mann-Whitney U-test ($\alpha = 0.05$) (Wilks 2011). In addition, results were averaged based on inflow regime, cross slope configuration, downspout configuration, and grate configuration with significant differences in efficiency between designs evaluated using the Mann-Whitney U-test ($\alpha = 0.05$).

To contextualize these experimental results with respect to design practices, a comparison of inlet spacing was conducted to understand the impact on design using the following equation for single slope bridges given by Young et al. (1993) as:

$$L_c = \frac{10000}{CiW_p}E \tag{7}$$

Where L_c = constant distance between inlets, C = the rational runoff coefficient, I = design rainfall intensity, and W_p = width pavement contributing to gutter flow. For this theoretical comparison of spacing, C was set to 0.9 as is typical for bridge decks (KDOT 2016), I was set to 152 mm/hr. as is a typical maximum design value (KDOT 2016), and W_p was set to 6.4-m which was the width scaled for the experimental model.

Sediment Cleanout

The second set of experiments was conducted to measure inlet erosion rate based on grate type (curved vane or rectangular bar) and flow intensity. The experimental set-up was modified to use only the first inlet, and experiments were extended from 3-minutes to 10-minutes each. At the inlet, a cohesive sediment mixture was packed underneath the grate to represent field conditions (Figure 3).

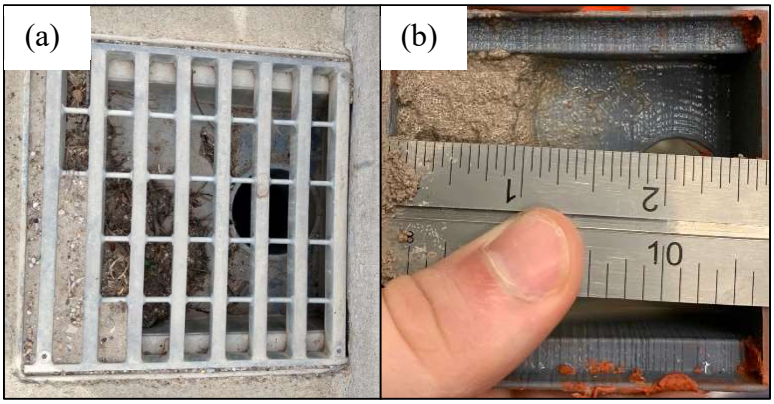

Figure 3. (a) Field image of a sediment-clogged inlet located near Topeka, KS, and (b) laboratory image from an experimental mix of clogging in a drain (with grate removed).

The mixture consisted of modeling clay, 0.5 mm silica, and water with composition percentages of 30%, 46%, and 24%, respectively. The wet density of the mixture was 2.04 g/cm^3 and the dry density was 1.99 g/cm^3. The experiments were conducted as described in Table 2 with three trials per combination. The average erosion rate (g/s) was measured by recording the loss of sediment mass over the 10-minute trials. Additionally, spread measurements were recorded at a location upstream and downstream of the inlet.

Table 2. Sediment cleanout experimental testing conditions.

Component	Number of Iterations	Iteration Types
Cross Slope	2	2%, 6%
Longitudinal Slope	4	0.5%, 1%, 2%, 4%
Inflow	3	0.68 m^3/h, 1.02 m^3/h, 1.59 m^3/h
Downspout shape	1	Square
Downspout Size	1	20 cm
Grate Type	2	Bar, Vane
Replicates	3	-
Number of Trials	144	

Experimental erosion data were contextualized with the literature by analyzing the relationship between dimensionless shear stress and transport with a comparison of natural mix types found in Walder (2015). For cohesive sediment, a dimensionless parameter for shear stress, $\widetilde{\Phi}$, and a dimensionless transport parameter, *R,* are defined as in Walder (2015):

$$\tilde{\Phi} = \frac{\varepsilon}{\rho_s(\tau_c/\rho)^{0.5}} \quad (8)$$

$$R = \frac{u_*^2 - u_{cr}^2}{u_{cr}^2} \quad (9)$$

Where ε = the sediment entrainment rate, ρ_s = the density of the sediment, ρ = the density of water, τ_c = the critical shear stress, u_* = the shear velocity, and u_{cr} = the critical shear velocity. Sediment entrainment was determined by van Rijn (1984) as $\varepsilon = M/At$ where M = the total mass of sediment lost, A = surface area, and Δt = the measurement period. The shear velocity was determined as $u_* = \sqrt{ghS}$, where g = gravity, h = the hydraulic radius, and S = the longitudinal slope. A critical shear stress of 0.014 Pa was used as determined from experimental testing of the upstream bed shear with a specific gravity of 2.04 and a dimensionless critical shear stress of 0.14. Analysis of erosion rates was conducted through averaging the results by grate type, inflow, and slope configuration with statistical significance determined using the Mann-Whitney U-test ($\alpha = 0.05$).

To inform design decision-making regarding optimal grate type as a function of flow regime, experimental results were applied to environmental conditions from eight sites across Illinois (IL) and Kansas (KS) by analyzing 15-minute precipitation data over a 10-year period (2000-2010) (NOAA 2021). The Kansas gauges were located in the towns of Iola, Lawrence, Smolan, and Wilson and the Illinois gauges were in Chicago, Danville, Illinois City, and Quincy. The rainfall data were used to categorize actual events into the three experimental inflow regimes (low, medium, and high). Cutoffs were determined through transforming the experimental inflow regimes to rainfall intensities (mm/hr.) by dividing by the deck area resulting in equivalent intensities of 94, 141, and 220 mm/hr. representing low, medium, and high intensities, respectively. Low-to-medium flow occurrences were defined as the number events in the range of 51 to 220 mm/hr. and high flow occurrences were events great than 220 mm/hr. Additionally, 10-

year 10-minute precipitation frequency gradients from NOAA Atlas 14 were plotted across Illinois and Kansas for further spatial analysis (Bonnin et al 2006; Perica et al. 2013).

Chapter 3: Results and Discussion

Hydraulic Efficiency of Inlet Designs

Experimental results showed that, on average, an increase in upstream inflow coincided with a decrease in hydraulic efficiency and a widening of roadway spread (Table 3). There was a noticeable, although nonsignificant ($p > 0.05$), difference in the average efficiency and spread between the two grate types with the curved vane grate showing higher efficiencies and lower spreads. This higher performance ranged from an increased efficiency of 1–3% and decreased spread of 2–4%, becoming more apparent at low and medium flow regimes. Additionally, analysis of how hydraulic performance was affected by downspout shape (circular vs square) and size (20 cm and 25 cm) indicated that larger downspout cross-sectional areas resulted in greater efficiency (Appendix C.3). Because the hydraulic efficiency results across all inflows and grate types were statistically indistinguishable, all data points were aggregated to assess the overall trend between efficiency and width-to-spread ratio.

Table 3. Hydraulic efficiency and spread width results presented as the average (±1σ) across inflows and grate designs.

Inflow	Number of Measurements		Average Efficiency (-)		Average Spread (cm)	
(m^3/h)	Bar Grate	Vane Grate	Bar Grate	Vane Grate	Bar Grate	Vane Grate
0.68	89	89	0.82 ± 0.22	0.84 ± 0.21	18.36 ± 11.24	17.64 ± 11.17
1.02	93	93	0.77 ± 0.22	0.80 ± 0.21	20.98 ± 11.91	20.21 ± 11.57
1.59	105	108	0.74 ± 0.25	0.75 ± 0.21	22.00 ± 12.77	21.48 ± 12.66

Experimental hydraulic efficiency (E) results showed a non-linear relationship with width-to-spread ratio (WT) (Figure 4a). Histograms of recorded efficiencies showed E ranging from 0.20 to 1.00 with a substantial portion (40%) of E values greater than 0.95. This result was expected as many experimental configurations produced flows that could be entirely captured by the deck inlet and thus had near-complete efficiency. Width-to-spread ratio results ranged from

0.15 to 1.00 with greater variability than *E*, but with some clustering at a *WT* of 0.95. At a *WT* of around 0.2, the minimum value of observed *E* drops sharply from around 0.5 down to 0.2 (Figure 4a). This drop could be due to flow splashing that occurs as high-momentum fluid enters the first slot of the grate, impacts the inlet pan, and redirects out of the last grate slot, and returns to the deck surface (Hammonds and Holley 1995). Hammonds and Holley (1995) demonstrated splashing through dye tracing whereas in these experiments it was observed through visual inspection. This could be the reason that the theoretical exponential efficiency curve (E_o) given by Eqn. 3 does not perfectly trend with the observed distribution (Figure 4a) of efficiency but does correlate reasonably well with measured data ($R^2 = 0.74$). After applying Eqn. 2 to correct efficiency for frontal (Eqn. 4) and side flow (Eqn. 5) ratios by grate type, the relationship improved ($R^2 = 0.78$) and examination of the grate corrected bounds (Figure 4a) shows that it covers approximately 40% of the data points with coverage across the overestimated area of the plot. However, the overall data trend still visually differed from the theoretical curve indicating the need for further analysis of the uncertainty between the experiments and the design equations.

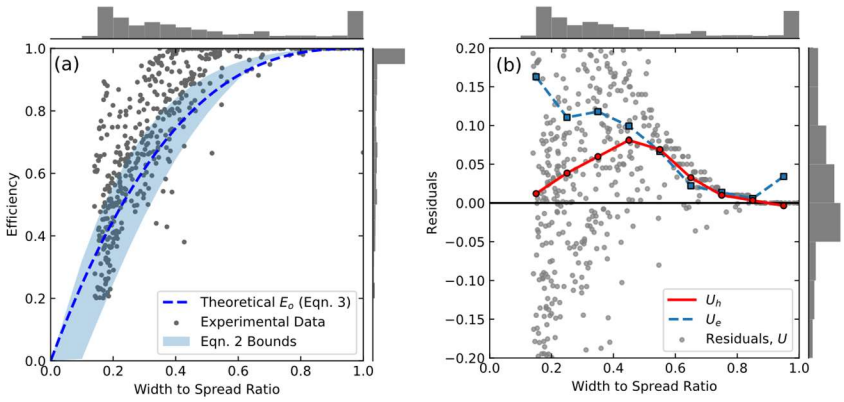

Figure 4. Hydraulic efficiency experimental data (n = 576) with comparison (a) between the theoretical curve and grate corrected maximum and minimum bounds (Eqn. 2). (b) The residuals between the experiments and the

theoretical design equation (Eqn. 2) or total uncertainty (U) are shown by the grey points with hydraulic uncertainty (Uh, red solid line) and experimental uncertainty (Ue, blue dashed line) plotted on top.

The experimental uncertainty (U_e) was higher for lower width-to-spread ratios that decreases as width-to-spread ratio increases (Figure 4b). This indicates that the high variability in low *WT* ranges was likely due to inconsistencies with the experiments, such as splash over velocity. The hydraulic uncertainty (U_h) was near zero at low *WT* ratios but increases before reaching a maximum of 0.08 at the 0.4 *WT* ratio and then decreases back to zero for higher *WT* ratios. This indicates that there was a consistent deviation between the experimental results and the theoretical design equations and implies the design equations underestimate efficiency. This was most pronounced at a *WT* of 0.4. While the visual results indicated a consistent underestimation of efficiency from the design equations, it should be noted that the U_h was not statistically different from zero for any of the bins shown in Figure 4b. This suggest that there was likely a discrepancy of up to 0.08 in the efficiency between the experiments and the theoretical design equations that could warrant an update in the design equations, but the experiments in this study lack the precision to define such an equation (Appendix C.2). Experimental uncertainty should be reduced in experiments by increasing the number of trial replicates per scenario with a singular inlet. This study examined multiple inlet in series which created varying approach discharges between inlets changing similarity between data points. Future experiments should focus on a single inlet across a larger number of inflow regimes similar to Holley et al. 1992.

Understanding the nature of design curves is important for designers as it can have adverse impacts on bridge deck drainage as the amount and spacing of inlets may be inadequate for storm events. To understand how efficiency selection impacts design and deck inlet spacing, a specific scenario of a bridge with a cross slope of 0.02, a longitudinal slope of 0.01, and a length of 610-m

with a design spread of 3.1-m was examined. Using the grate-adjusted exponential curve (Eqn. 2), calculated efficiencies were 0.52 for both bar and vane grates, respectively, which correspond to a constant inlet spacing of 144-m. The design equations used to derive this spacing estimates were also developed empirically from experimental results (Izzard 1950) and thus also susceptible to design uncertainty (U_e). The experimental uncertainty applied to this design scenario would be 0.16 as seen in Figure 4b. The efficiency prediction from the lower uncertainty bound would equal 0.36 which corresponds to a required spacing of 101-m. In this case, the current design standards (Eqns. 2 and 3) would underestimate the required number of inlets by two. The net result is that flow spread onto the roadway would not meet design criteria and could lead to increased risk of traffic hazards from hydroplaning. However, the efficiency prediction from the higher uncertainty bound would be 0.68 with a required spacing of 191-m indicating the number of inlets would be overestimated. In this case, correct estimation could reduce cost and eliminate potential issues related to structural design as less inlets would be needed compared to theoretical values. The results of experimental uncertainty on design highlight the importance of correctly estimating the limitations to efficiency based on grated inlet performance characteristics to optimize cost and safety when derived from experimentation.

Results from this study and other experimental studies (Holley et al. 1992; Schalla 2017; Mohammad, 2018) have shown discrepancies between experimental results and standard roadway drainage guidance indicating that further investigation is needed to verify design predictions. However, experimental modeling is cost and time prohibitive for non-research-based designers without access to laboratories and equipment. Potential future implementations of computational fluid dynamics (CFD) models could provide a low-cost, accurate method for estimating efficiency (Cai and Huang 2021). A study performed by Fang et al. (2010) examined the use of CFD on

curbed inlet openings to experimental results from Hammond and Holley (1995). Their findings indicated that an advanced CFD model (e.g., FLOW-3D) can simulate complex shallow flow accurately and could be used as a virtual laboratory to predict inlet efficiencies for complex geometries. This is further supported by Li et al. (2019) and Cai and Haung (2021), who used CFD models (FullSWOF_2D and ANSYS fluent, respectively) to examine complex roadway geometries to determine accurate capture efficiency and water depth estimates. As a future step, the outputs of this experimental work could be used to calibrate and validate an aforementioned CFD model to further elucidate dominant processes controlling bridge deck drainage.

Overall, this experimental testing showed similar performance between tested grate types, indicating that grate type is not a sole control on inlet efficiency. However, curved vane grates had slight, but non-significant, improvements in hydraulic efficiency over rectangular bar grates. Further, these experiments indicated that standard design curves using exponential efficiency curves may not accurately estimate variability of hydraulic efficiency. The impacts to design from these findings are relevant for both safety and cost. Designers should consider performance characteristics from manufactures, experimental data, or implement numerical models if possible.

Sediment Cleanout Potential of Grates

The differences in sediment cleanout between bar and vane grates were starker than differences in hydraulic efficiency between the grate types (Table 4). In general, erosion rate tends to increase with flow rate. This was true for all bar grate flow scenarios with erosion rates at low, medium, and high inflow regimes of 0.045 (±0.015), 0.056 (±0.023), and 0.067 (±0.045) g/s, respectively. However, this was not the case for vane grates as erosion increased initially from low (0.049 ± 0.022) to medium (0.075 ± 0.059) inflows, but then decreased at high flows (0.059 ±

0.023). Statistical comparison of the inflow averages found no statistically significant difference ($p > 0.05$) but was mainly attributed to the small experimental sample size per inflow (n=24).

Table 4. Erosion rate presented as the inflow average (±1σ) for each grate designs (n = 24 for each inflow).

Inflow (m^3/h)	Erosion Rate (g/s)	
	Bar Grate	Vane Grate
0.68	0.045 ± 0.015	0.049 ± 0.022
1.02	0.056 ± 0.023	0.075 ± 0.059
1.59	0.067 ± 0.045	0.059 ± 0.023

At low-to-medium flows, it is hypothesized that the vane grate is able to guide the water into the inlet as its design has curved bars, (Appendix G) transitioning from horizontal to vertical, that aid gravity in changing the direction of gutter flow to improve erosion rates. Observations from video recordings of the experiments found that at low-to-medium flows water could be seen traveling along the vane and diverted into the inlet along the vertical side of the cohesive sediment more efficiently compared to the bar grate which allowed more flow to bypass horizontally over the sediment material supporting the results in Table 4. However, at higher flows, when grates are submerged, it is hypothesized that the curvature of the vanes may cause an obstruction in the vertical flow path of water toward the downspout pipe, limiting erosion potential. Grate-splashover velocity relationships found in Johnson and Chang (1984) support this idea as a vane grate was shown to have more splashover compared to a bar grate for large gutter flows. This explanation is plausible as the rectangular bar grate, with its bars parallel to potential vertical flow paths, had improved cleanout over the curved vane grate at high flows. The experiment shows how bridge configuration and inflow can affect the movement of debris based on grate type. Further breakdown by slope configuration is discussed in Appendix C.4.

Experimental erosion data from the bridge deck setup was compared to data from Walder (2015) for a range of sediment types (Figure 5). The erosion comparison shows that the bar and vane grate results were on the higher end of values reported for other cohesive sediment. Walder (2015) conducted his analysis with data from erosion flumes, hole-erosion test, and submerged jet test with various ranges of flow and pressure whereas these experiments were performed in an open channel with comparatively low pressure and flow rate gradients.

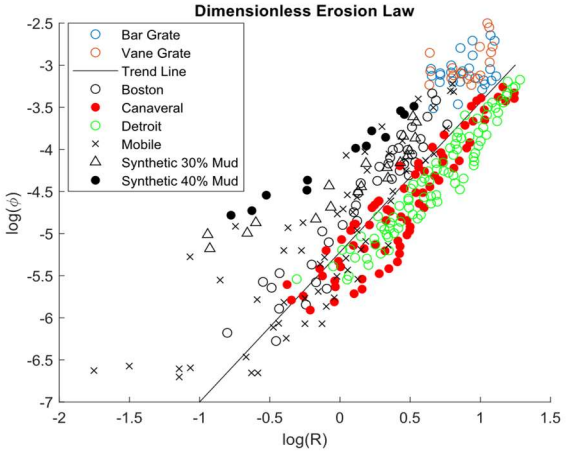

Figure 5. Dimensionless erosion rate (ϕ) and transport stage (R) relationship of bar and vane grate erosion tests (blue and orange open circles, respectively) plotted alongside data aggregated from other cohesive studies (Walder, 2015).

Further, the comparison erosion studies were conducted for one-dimensional, uniform flow whereas this experiment had considerable two- and three-dimensionality due to downspout flow abstraction and lateral overflow to the grate. Additionally, Walder (2015) shows that this experimental mixture performs similar to sediment form the Boston channel and Detroit River with clay sized fractions of 42% and 31%, respectively. The comparison in data indicates that further type of sediment is needed specifically based on location as material mixture can greatly impact the results as the percentage of clay fractions in Walder's data ranges from 0% to 42%. However, the compression of data applying the cohesive sediment parameters provided in Walder (2015) provide a future reference to compare data. The results of these experiments highlight a

need to further consider the relationship between grate type and clean out potential as debris accumulation is one of the most prominent issues in the field (Gómez et al. 2019).

The movement of debris and the choice of what grate type to utilize in design are affected by flow and sediment dynamics, which are influenced by geographic bridge location. Precipitation analysis across eight sites in Kansas and Illinois provides support for selecting grate type based on expected storm intensities (Figure 6).

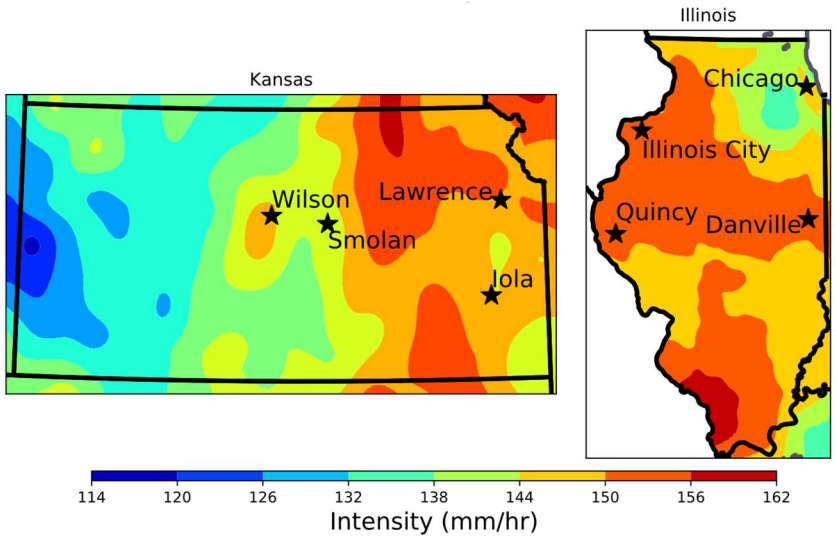

Figure 6. Rainfall Intensity gradient for 10-year 10-minute design storm as provided by NOAA Atlas 14.

Each site's unique storm intensity characteristics resulted in different recommendations for the type of grate to use in design. For the four sites in Kansas, events falling within the high-flow regime are the predominant storm types (Table 5) thus suggesting that bar grates are more suitable for effective design given that the results showed they performed better under these conditions (Table 4). For the Illinois sites of Chicago, Danville, and Illinois City, low-to-medium intensity events are temporally more common, thus designers should utilize curved vane grates as they perform best under low and medium inflow rates. Incidentally, ILDOT was the only DOT to not report issues related to debris clogging and to primarily use curved vane grates (Table 6, Appendix A.3), which provides some credence to the geospatial precipitation analysis and experimental

efficiency results. For Quincy, IL, the breakdown of events indicate that it would be advantageous to use the bar grate as it could remove sediment as high intensity events are common. Adversely, examination of spatial intensity maps in Figure 6, shows that Illinois has higher overall intensities whereas Kansas has greater variability in rainfall intensities. Design storms as shown in Figure 6 are typically used to determine design intensity for a location. However, designers should note that surface runoff generation is directly associated with temporal patterns in rainfall intensity which drives sediment yield through rainfall impact and scour (Tao et al. 2017). It should be noted that precipitation might not be the sole driver of sediment removal as sediment mixture is location dependent as discussed previously. Further investigation into debris-grate relationships should examine the impact of location specific soil type, land use, and traffic patterns to address other factors that may control erosion potential. Overall, with the creation of debris removal data, designers could easily integrate precipitation analysis into their designs as rainfall intensity is already used to determine spacing.

Table 5. Experimental intensity occurrence at 8-gauge locations for 2000-2010 from NOAA CDO precipitation data.

Location	Station ID	Less than Test Flow (%)	Low-to-Medium Flow (%)	High Flow (%)	Optimal Grate Type
Iola, KS	COOP:143984	25.1	30.2	44.7	Bar
Lawrence, KS	COOP:141612	24.3	35.7	40.0	Bar
Smolan, KS	COOP:147551	24.6	33.0	42.4	Bar
Wilson, KS	COOP:148946	26.3	28.9	44.8	Bar
Chicago, IL	COOP:111577	29.8	37.1	33.1	Vane
Danville, IL	COOP:112140	17.1	51.5	31.4	Vane
Illinois City, IL	COOP:114355	21.5	40.5	38.0	Vane
Quincy, IL	COOP:117077	26.9	30.9	42.2	Bar

Further studies are needed to understand relationships between grate types and sediment transport to establish specific design guidance. Sediment buildup and transport processes are highly variable with spatial heterogeneities across drainage areas (Naves et al. 2020), which needs to be explored further for developed structures. Along with determining sediment removal

relationships, similar experiments can also be used to quantify a clogging coefficient to provide optimized safety factors for design based on debris patterns as performed by Guo and Mackenzie (2012) and Gomez et al. (2019). This would allow designers to better predict field values of efficiency especially when coupled with specific design efficiency curves. Additionally, two-dimensional sediment transport or CFD-DEM models which have been successful in complex natural environments (Fang et al. 2017; Shobe et al. 2017; Sun et al. 2017) could be coupled with experimental modeling to provide framework for estimating routing of sediment through drainage systems. Overall, accounting for debris removal would help to alleviate costs due to maintenance as well as bridge deck degradation which can help to prolong bridge structures for the future and allow for better bridge performance (Ghodoosi et al. 2018; Kim et al. 2020).

Chapter 4: Conclusions

Overall, the goals of this study were to assess the hydraulic efficiency of grate inlets for bridge decks as well as understand the relationship between inlet design and sediment removal. The main hydraulic efficiency finding was that the experimental uncertainty is largest for low width-to-spread ratios and that the design equation underestimates efficiency by up to 0.08. However, the experimental uncertainty was too large to justify creating an updated design equation. Yet, these results still highlight the importance of understanding the uncertainty of inlet characteristics as overestimating spacing can affect motorist safety and underestimating can affect cost. The second major finding was that curved vane grates had greater sediment cleanout rates at lower flow rates whereas rectangular bar grates performed better at high inflows. Comparing the experimental inflows with rainfall over a ten-year period at eight sites showed how the distribution of precipitation events can be compared to help in deciding between grate types if debris removal performance is known. Designers should further investigate the type of grate used for an area depending on the amount of expected debris and rainfall frequency to help alleviate issues of clogging which decrease the capacity of drainage and increase the cost of maintenance. Overall, the results of this study contribute added guidance for bridge deck drainage system design, which could help alleviate the risks of hydroplaning and improve roadway safety.

References

Bakr, A.R., Fu, G.Y., and Hedeen, D. (2020). “Water quality impacts of bridge stormwater runoff from scupper drains on receiving waters: A review.” *Science of The Total Environment,* 726, p.138068.

Bonnin, G.M., Martin, D., Lin, B., Parzybok, T., and Yekta, D.R. (2006). "NOAA atlas 14 volume 2 version 3, precipitation-frequency atlas of the united states, ohio river basin and sorrounding states." *NOAA*, National Weather Service, Silver Spring, MD.

Cai, W. and Huang, L. (2021). “Quantitative research based on parametric simulation of waterlogging on bridge decks.” *IOP Conf Ser Earth Environ Sci,* 638:012060. doi: 10.1088/1755-1315/638/1/012060

Fang, H.W., Lai, H.J., Cheng, W., Huang, L., and He, G.J. (2017). “Modeling sediment transport with an integrated view of the biofilm effects.” *Water Resour. Res. 53:7536–7557. doi: 10.1002/2017WR020628*

Fang, X., Jiang, S., and Alam, S.R. (2010). “Numerical simulations of efficiency of curb-opening inlets.” *J. Hydraul. Eng.,* 136:62–66. doi: 10.1061/(asce)hy.1943-7900.0000131

Ghodoosi, F., Abu-Samra, S., Zeynalian, M., and Zayed, T. (2018). "Maintenance cost optimization for bridge structures using system reliability analysis and genetic algorithms." *J. Constr. Eng. Manag.,* 144:04017116. doi: 10.1061/(asce)co.1943-7862.0001435

Gómez, M., Parés, J., Russo, B., Martínez-Gomariz, E. (2019). "Methodology to quantify clogging coefficients for grated inlets. Application to SANT MARTI catchment (Barcelona)." *J. Flood Risk Manag.,* 12:1–10. doi: 10.1111/jfr3.12479

Guo, J., and Mackenzie, K., (2012). "Hydraulic efficiency of grate and curb-opening inlets under clogging effect." *Research Report CDOT-2012-3.* DTD Applied Research and Innovation

Branch, Colorado Department of Transportation.

Hammonds, M.A., and Holley, E. (1995). “Hydraulic characteristics of flush depressed curb inlets and bridge deck drains.” *Research Report 1409-1.* Center for Transportation Research, The University of Texas at Austin.

Holley, E.R., Woodward, C., Brigneti, A., and Ott, C. (1992) “Hydraulic characteristics of recessed curb inlets and bridge drains.” *Research Report 1267-1F.* Center for Transportation Research, The University of Texas at Austin.

Izzard, C.F. (1946). "Hydraulics of runoff from developed surfaces." *In Proceedings of the 26th Annual Meeting of Highway Research Board National Research Council*, Washington, DC, USA, pp. 129–150.

Izzard, C.F (1950). "Tentative results on capacity of curb opening inlet." *Research Report No. 11-B; Highway Research Board*, Washington, DC, USA, pp. 36–51.

Johnson, F.L., and Chang, F. (1984). “Drainage of highway pavements.” *Hydraulic Engineering Circular No.12.* Federal Highway Administration.

Kansas Department of Transportaiton (KDOT), (2016). *Design manual volume III - bridge section.* Topeka, KS.

Kim, K.H., Nam, M.S., Hwang, H.H., and Ann, K.Y. (2020). "Prediction of remaining life for bridge decks considering deterioration factors and propose of prioritization process for bridge deck maintenance." *Sustain.,* 12:1–25. doi: 10.3390/su122410625.

Li, X., Fang, X., Chen, G., Gong, Y., Wang, J., and Li, J. (2019). "Evaluating curb inlet efficiency for urban drainage and road bioretention facilities." *Water,* 11:1–18.

McEnroe, B. M., Wade, R. P., Smith, A. K. (1999). "Hydraulic performance of curb and gutter inlets." Report No. K-TRAN KU-99-1.

Muhammad, M.A. (2018). "Interception capacity of curb opening inlets." Ph.D. thesis, University of Texas.

NOAA, (2021). "National centers for environmental information data available on the world wide web (NOAA Climate Data Online)." https://www.ncdc.noaa.gov/cdo-web/. (Accessed 4 February 2021).

Naves, J., Anta, J., Suárez, J., and Puertas, J. (2020). "Hydraulic, wash-off and sediment transport experiments in a full-scale urban drainage physical model." *Sci. Data.*, 7:1–13. doi: 10.1038/s41597-020-0384-z.

Perica, S., Martin, D., Pavlovic, S., Roy, I., St. Laurent, M., Trypaluk, C., Unruh, D., Yekta, M., and Bonnin, G. (2013). "NOAA atlas 14 volume 8 version 2, precipitation-frequency atlas of the united atates, midwestern states." *NOAA*, National Weather Service, Silver Spring, MD.

Schalla, F.E., Ashraf, M., Barrett, M.E., and Hodges, B.R. (2017). "Limitations of traditional capacity equations for long curb inlets." *Transp. Re.s Rec.,* 2638:97–103. doi: 10.3141/2638-11.

Shobe, C.M., Tucker, G.E., and Barnhart, K.R. (2017). "The space 1.0 model: a landlab component for 2-d calculation of sediment transport, bedrock erosion, and landscape evolution." *Geosci. Model Dev.* 10:4577–4604. doi: 10.5194/gmd-10-4577-2017.

Sun, R., Xiao, H., and Sun, H. (2017). "Realistic representation of grain shapes in cfd-dem simulations of sediment transport with a bonded-sphere approach." *Adv. Water Resour.,* 107:421–438. doi: 10.1016/j.advwatres.2017.04.015.

Tao, W., Wu, J., and Wang, Q. (2017). "Mathematical model of sediment and solute transport along slope land in different rainfall pattern conditions." *Sci. Rep.*, 7:1–11. doi: 10.1038/srep44082.

Qian, Q., Liu, X., Barrett, M.E., and Charbeneau, R.J. (2016). "Physical modeling on hydraulic performance of rectangular bridge deck drains." *Water (Switzerland)*, 8:1–11. doi: 10.3390/w8020067

van Rijn, L.C. (1984). "Sediment pick-up functions." *J Hydraulic Eng,* 110:1494–1502.

Walder, J.S. (2015) "Dimensionless erosion laws for cohesive sediment." *Journal of Hydraulic Engineering.* doi: 10.1061/(asce)hy.1943-7900.0001068.

Wilks, D.S. (2011). Statistical methods in the atmospheric sciences, 3rd ed., ISBN: 978-0-12-3850225-5.

Young, G.K., Walker, S.E., and Chang, F. (1993) “Design of bridge deck drainage.” *Hydraulic Engineering Circular No. 21.* Federal Highway Administration. Washington, D.C.

Appendices

Appendix A: Survey for Departments of Transportation

A.1 Survey Intent

Upon completing the literature review of bridge deck drainage further investigation was needed to understand what the most common design procedures, drain types, grate types, issues, and solutions to drainage issues were used to better inform the design of the experiment. A survey was sent out to all fifty Departments of Transportation to assess the most common design methods, inlet types, as well as information relating to inlet clogging (see Appendix A.2 for questions asked). A response was received from 22 states and the most relevant information related to field issues, drain design, and design guidance are shown in Appendix A.3.

A.2 Survey Questions

DOT Bridge Deck Drainage Survey

DOT State:_____

DOT Engineer Name:_____

Phone: _____ Email: _____

Questionnaire Section

1) Inlet Type Used: Scupper Grated Inlet Other (Please Specify): _____

2) Typical Inlet Size_____

3) Material type of Inlet: _____

4) Inlet Manufacture: _____

5) What are the Most common issues that affect the bridge deck drainage (i.e. clogging, debris, collection system, capacity, etc.):_____

_____

_____

_____

Solutions:_____

6) What type of data sets are available? Are maintenance records or accident reports available?

_____

_____

_____

_____

7)What type of collection system is used (i.e. 8" fiberglass, closed system)? Are there any problems with the system such as clogging that affect the drainage as a whole?

_____

_____

_____

_____

8) What type of grate system is commonly used? What is the efficiency of the grate?

_____

_____

_____

9) For design, what factor is used to account for clogging? _____

10) What Reference Document is used for Design: HEC-12 HEC-21 HEC-22 Other:_____

11) Is inlet spacing based solely on design or is there a standard spacing used? _____

_____

_____

12) Additional Provided Reference Material (Details of Typical Inlets, design documents, etc.):_____

_____

_____

A.3 Survey Results

Analyzing the design related results of the survey, 14 of the 22 states use HEC-21 for design guidance whereas only Nevada reported using HEC-12 as is used by the state of Kansas. The common drain types used were scuppers, grated inlets, and slotted openings. The states that reported using scuppers include Alaska, Connecticut, Delaware, Georgia, Illinois, Louisiana, Maryland, Nevada, New Hampshire, Ohio, Pennsylvania, South Dakota, and West Virginia. Arkansas, Colorado, Delaware, Illinois, Minnesota, Nebraska, Nevada, New York, and Oregon each reported using a grated inlet. Slotted openings were specified as common in Hawaii and North Carolina. The type of grate varies by state with the listed types being bar, vane, cross hatch, and none. The vane grate is used by Colorado, Illinois, and West Virginia. The two states using the cross-hatch grate are Minnesota and New Hampshire. Only South Dakota reported using no grate. The typical size of drains varied with the smallest being a 10-cm scupper used by South Dakota and the largest a 1.1-m x 0.46-m grated inlet used by Nebraska. Each state follows similar guidelines but uses vastly different inlet and grate combinations. This indicates that investigation of hydraulic performance curves should be examined and compared to standard design curves as designs are not standardized to check for accuracy.

Regarding issues related to bridge deck drainage, 21 of 22 states varying in region of the U.S. reported that the most common issue plaguing bridge deck drainage is clogging of the drain or downspout in some capacity independent of size and type of drain used. The responses to this issue vary with a common answer being to have routine maintenance or no solution. Colorado and Indiana indicate that they design for clogging as a solution. Maryland's DOT listed to design bridges with higher longitudinal slope as a potential solution. Another unique response was by Ohio's DOT which indicated that they lower the speed limit and increase the shoulder width. Based

the response from an engineer at ILDOT, it was indicated that they most commonly used a curved vane grate and did not have any issues with clogging. Four states (Indiana, Louisiana, Minnesota, and Nevada) implemented a safety factor to account for clogging whereas most other areas reported that design was based solely on the assumption that inlets are clean. Indiana, Louisiana, and Minnesota assumed a safety factor of 2 (or 50%) whereas Nevada set multiple clogging factors with a sag curve requiring 50%, 25% for designated high debris areas, and 10% for everywhere else.

Overall, the survey responses highlighted a need to understand the impact of drain and grate type on efficiency due to the vast range of combinations to verify current performance curves are adequate. Additionally, almost every state surveyed had issues with clogging and literature on this subject is lacking. Therefore, indicating a need to examine the effects of debris on performance as well as to help understand if a grate type (ILDOT vane) can potentially reduce the amount of debris.

Full Results:
https://docs.google.com/spreadsheets/d/1AayTNZz1O1fXVpROyfxkCCiLzOKv2mlWrt-VqSltGKM/edit?usp=sharing

Table 6. Study related results of Bridge Deck Drainage Survey

State	Drain Type	Typical Size	Grate Type	Common Issues	Solutions to Issues	Clogging Factor	Design Reference
Alaska	Scuppers	0.15-m to 0.20-m	Varies	Clogging	Routine Maintenance	None	HEC-21
Arkansas	Grated Inlet	0.61-m x 0.36-m	Bar	Clogging	Routine Maintenance	None	HEC-21
Colorado	Grated Inlet	Varies	Vane	Clogging	Design for clogging/ increase Maintenance	None	HEC-21
Connecticut	Scupper	0.61-m x 0.61-m	Bar	Clogging	Routine Maintenance	None	HEC-21
Delaware	Scupper and Grated Inlet	0.30-m x 0.30-m	N/A	Clogging	No solution	None	HEC-22
Georgia	Scupper	0.10 dia.	Bar	Capacity, Clogging	No solution	None	HEC-21
Hawaii	Slotted Openings	0.91-m x 0.61-m	Bar	Clogging	Add drains, Maintenance	Location Dependent	HEC-12
Illinois	Scupper and Grated Inlet	0.3-m x 0.3-m 0.3-m x 0.6-m	Vane	No issues	N/A	None	HEC-21
Indiana	Grated Inlet	0.51-m x 0.48-m	Bar	Clogging	Using Clogging Factor	Assume 50% Clogged	Indiana Design Manual
Louisiana	Scupper	0.20-m dia.	N/A	Clogging	Routine Maintenance	Safety Factor of 2	HEC-21
Maryland	Scupper	Varies	Bar	Clogging	Design bridge with higher longitudinal slopes	None	HEC-22
Minnesota	Grated Inlet	0.43-m x 0.43-m	Cross hatch	Clogging	Avoid underdeck pipe system	Assume 50% Clogged	HEC-22
Nebraska	Grated Inlet	1.04-m x 0.43-m	Bar	Clogging	Routine Maintenance	None	HEC-21
Nevada	Scupper and Grated Inlet	0.61-m x 0.91-m 0.23-m x 0.46-m	Bar	Designing for maintenance	Avoid Deck Drains	Assume 50% for Sag, 25% for high debris, 10% all other	HEC-12, HEC-21, HEC-22
New Hampshire	Scupper	0.46-m x 0.15-m 1.22-m x 0.38-m	Cross hatch	Rusting, Clogging	Increase Routine Maintenance	None	HEC-21
New York	Grated Inlet	0.56-m x 0.43-m	Bar	Clogging, Downspout disconnection	Use bridge washing program	None	HEC-21
North Carolina	Slotted Openings	0.15-m dia.	N/A	Clogging	Paved approach shoulders	None	HEC-21
Ohio	Scupper	Varies	Varies	Clogging	Widen shoulders, Reduce speed limits	None	OHDOT Manuals
Oregon	Grated Inlet	0.81-m x 0.36-m	Bar	Clogging	Routine Maintenance	None	ODOT Hydraulics Design manual
Pennsylvania	Scupper	0.53-m x 0.46-m	Bar	Clogging	Routine Maintenance	None	HEC-22
South Dakota	Scupper	0.10-m dia.	Open	Capacity	More or Larger Inlets	None	HEC-21
West Virginia	Scupper	0.15-m or 0.20-m dia.	Bar or Vane	Clogging	Increase Routine Maintenance	Designers Discretion	HEC-21

Appendix B: Literature Review of Related Studies

A literature search performed for this study found that few references were available specifically related to bridge deck drainage outside of the previously mentioned HEC references. Much of the existing literature on roadway drainage is for street drains which operate under much larger flow regimes. The primary references for this study (Holley et al. 1992; Hammonds and Holley 1995; Qian et al. 2012) were all performed for the Texas Department of Transportation (TXDOT) and each used a variation of the same model. The experimental design and procedure were based on their collective works.

B.1 Qian et al. 2015

Qian et al. (2015) researched the hydraulic performance characteristics of a new rectangular deck drain for Texas DOT. The size of the tested rectangular drain inlets were 10-cm x 20-cm and 15-cm x 20-cm. The study compared the Federal Highway Association slotted drain method and grate inlet method from HEC-21 to experimental results to determine if the method could be used for design with the new 10-cm x 20-cm. The overall result was that the slotted drain method underestimated the capacity while the grate inlet method overestimated capacity for longitudinal slopes less than 0.005. This required the development of a new equation specifically for the 10-cm x 20-cm drains to replace Eqn. 1 shown below as:

$$Q_{c100\%}=k_{100\%}(N_m(L_g+W))^{16/7} n^{9/7} \frac{S_x^{0.7136}}{S^{0.4046}} \quad (10)$$

Where $Q_{c100\%}$ = 100% of gutter flow captured, N_m = the number of drains required, and $k_{100\%}$ = 1.4598. These values were developed from the statistical analysis of results for fitted coefficients.

The set up consisted of testing a 3.2-m-wide bridge deck model that was 19.5-m-long in length consisting of a plywood deck with two curbs reinforced by angle iron. The deck was coated

with granular material and resin to provide a correct Manning's roughness coefficient. The deck contained 2x6 joists with a W12x16 steel lifting beam and two 18.3-m long W18x35 steel beams. Two five-ton hoists were used to be able to adjust the cross slope and longitudinal slope with the downstream end sitting on a support for adjustment. The deck drains were made of plexiglass and placed 0.46-m apart with the ability to close off drains in order to able to use from 1 to 5 in a series. The first deck drain was placed 14.2-m from the headbox to allow for flow to simulate sheet flow on a deck. A 1.5-m head box was used at the upstream end of the structure using two water pumps to discharge directly onto the bridge.

A total of 586 tests were completed for the 10-cm x 20-cn drains and 236 tests on the 15-cm x 20-cm drain. The main variables were the capture discharge, the approach discharge, the flow curb depth, the number of drains, cross slope, longitudinal slope, drain length, and drain width. Each of these were used to analyze Izzard's equation (Eqn. 1) for discharge and modify it so that the Eqn. 10 could be developed. Their study provided the main concepts critical to setting up an experiment for this study.

B.2 Holley et al. 1992

Holley et al. (1992) performed tests on curb inlets and bridge decks to determine the hydraulic characteristics at various flow conditions and geometries. The objective for the bridge deck drains was to test two different types of inlets and develop design equations for bridge deck drains. The two drains were the same except that the orientation was changed. The drains each consisted of the use of a piping system which was a 0.152-m 90° PVC elbow at the outlet pipe. A scale model of ¾ scale was used in this experiment (Figure 7).

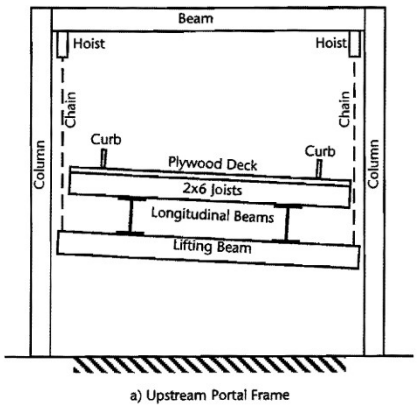

Figure 7. Experimental model diagram from Figure 3.1a of Holley et al. 1992.

Model scaling required that the model and the prototype must have hydraulic similitude determined by the following ratios based on the length ratio (Λ_r):

$$V_r=\Lambda_r^{1/2} \tag{11}$$

$$Q_r=\Lambda_r^{5/2} \tag{12}$$

$$n_r=\Lambda_r^{1/6} \tag{13}$$

Where V_r = the velocity ratio, Q_r = the discharge ratio, and n_r = the ratio of Manning's roughness coefficient. The grain size needed to achieve the required Manning's n was determined by the following relationship presented by the following equation:

$$n=0.041d_{50}^{1/6} \tag{13}$$

Where d_{50} is the median sand grain size. In this study a grain size of 2-mm was used. These equations were used to help with the scaling aspect in this study.

The first important result presented by Holley et al (1992) was the efficiency curves for curbed inlets on roadways. They represented their data (Figure 8) similar to the efficiency curve provided by Johnson and Chang (1984) which helped guide the representation of results. The experimental results for the curbed inlets found that the efficiency curve provided by Eqn. 3 over

estimated efficiency (dotted line in Figure 8) as their results showed efficiency was much less and represented by a cubic function for the width to spread ratio.

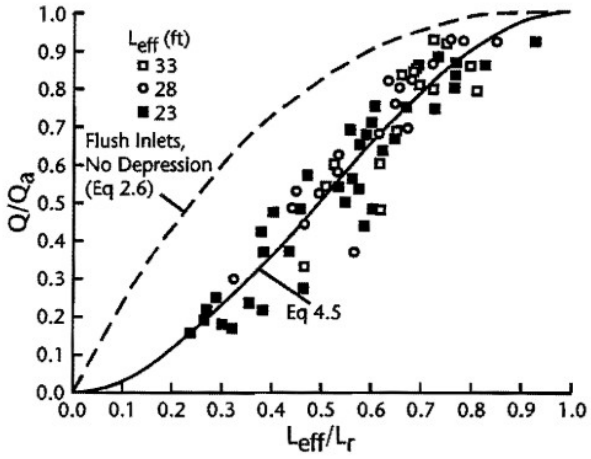

Figure 8. Figure 4.3 from Holley et al. 1992 showing efficiency results for curb inlet experiments.

One of the other most important aspects of their research specifically related to bridge deck drains was the classification of the drain behavior between low flow control, weir/orifice control where the inlet capacity is controlled by the grate as weir control or by the inlet downspout as orifice controlled, and high flow in which the capacity is limited by the back pressure of the pipe system. The results of their experiments found that the efficiency was much higher for weir/orifice control as opposed to pipe system controlled. For a configuration of longitudinal and cross slopes, increased flow rate in the weir/orifice control regime caused an increase in captured flow. The same increase in flow rate in the piping system control regime caused less increase in captured flow. Additionally, the authors found that the weir control section happens when water is able to freely fall into the pan whereas orifice control only occurs when the drain pan is full. These findings helped us contextualize the results of this study related to the control of inlet capacity.

B.3 Hammond and Holley 1995

Hammond and Holley (1995) study was similar to that of Holley et al. (1992) performing experiments using the same model and scaling on curbed inlets and bridged deck drains with the addition of another drain type (Figure 9). The experimental work on deck drains (Chapter 9) aimed at examining the capacity of the three different drain types with test being performed across a range of discharges (0.01 to 0.07 m^3/s) with longitudinal slopes ranging from 0.004 to 0.06 and cross slopes ranging from 0.0208 to 0.0417. The authors found that when the downspout was opposite of the bridge curb that it had a decreased capacity as opposed to the downspout next to the curb. The additional drain type examined shown in Figure 9 showed a greater hydraulic capacity compared to the other designs due to the larger pan, inclined vane grate, and larger orifice (downspout). The authors determined an empirical formula for estimating capture discharge for each drain type. They found that capture discharge was a function of the normal depth, longitudinal slope, and cross slope. For the drain type shown in Figure 9 the following equation was determined:

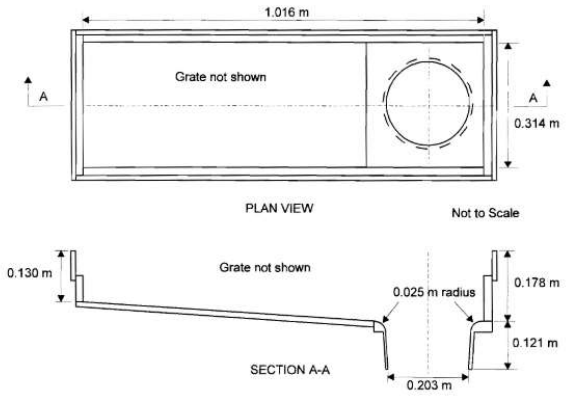

Figure 9. Drain 4 Pan from Figure 5.8 of Hammonds and Holley 1995.

Appendix C: Additional Experimental Results

The experimental data for the efficiency and sediment transport tests can be found listed in Appendix E and Appendix F, respectively. A total of 576 tests were completed for the efficiency tests where three trial replicates were used for each configuration listed in Table 1. Of this total 24 tests were done for each configuration of inlets (i.e. 20-cm round with a bar grate, etc.). The primary variables were the captured flow (Q_c), the approach flow (Q), the spread width upstream of an inlet (T), the cross slope (S_x), the longitudinal slope (S), and the drain length (W). The drain length for all drains was 0.61-m or scaled to 6.9-cm. The approach flow was calculated using a continuity mass balance where approach flow at the first inlet was the sum of captured flow and total captured flow minus the captured flow at each upslope inlet for the rest of the inlets to the last inlet capturing water ensuring that efficiency could not exceed one.

For the sediment removal test a total of 144 tests were done using a single inlet (20-cm square) where the breakdown was 72 for the bar and vane grate apiece. Again, three trial replicates were done at each flow rate, cross slope, and longitudinal slope. The main variables were the weight of sediment before (w_b) and after (w_a) each run, time of experiment (t), inflow rate (Q), the cross slope (S_x), the longitudinal slope (S), and the area of the removable sediment (A).

C.1 Bridge Deck Roughness Coefficient

The scaled Manning's coefficient of 0.012 was validated experimentally. The standard Manning's equation for rectangular channels was utilized by setting the cross slope to zero on the model and measuring the flow depth for each configuration of discharge and longitudinal slope. Depth measurements were taken at three separate locations and averaged for each trial. Additionally, three trials were done for each configuration of longitudinal slope and discharge. The longitudinal slopes were S = 0.5%, 1%, 2%, 3%and 4%. The discharges used were based on

the number of turns of the inflow valve with equivalent values of 1.8, 2.3, and 4.5 m^3/hr. The average was taken across the discharge range as shown by the red line in Figure 10. The grey, blue, and orange dotted lines represent the Manning's n across the slope range for discharges of 1.8, 2.3, and 4.5 m^3/hr, respectively. The average Manning's coefficient across all values was equal to 0.012 with a standard deviation of 0.002. These results indicate that for the range of longitudinal slopes and inflows the coating consistently represents the real-world conditions.

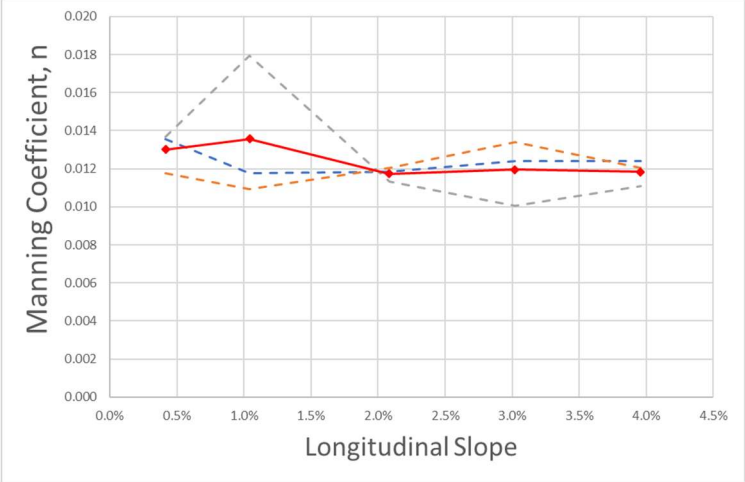

Figure 10. Manning's n Coefficient as a function of Longitudinal slope with discharge setting of 1.8 m^3/hr. (grey dotted lined), 2.3 m^3/hr. (blue dotted line), and 4.5 m^3/hr. (orange dotted line) on the inflow dial. The solid red line indicates the average based on the longitudinal slope.

C.2 Efficiency and Spread Measurement Uncertainty

To help quantify the uncertainty between experimental runs, the deviation for efficiency and spread were determined as the value for the trial with the average for the three trials removed. This centered the data around a mean of zero. Histograms were used to assess the distribution fit for both variables. The efficiency variation had an approximate normal distribution fit as seen in Figure 11. The deviation in efficiency was very small (1.9%) with a 95% level of uncertainty at

+/-3.8%. The small deviations allowed for us to assume it was appropriate to examine the statistical difference in efficiency between inlet configurations.

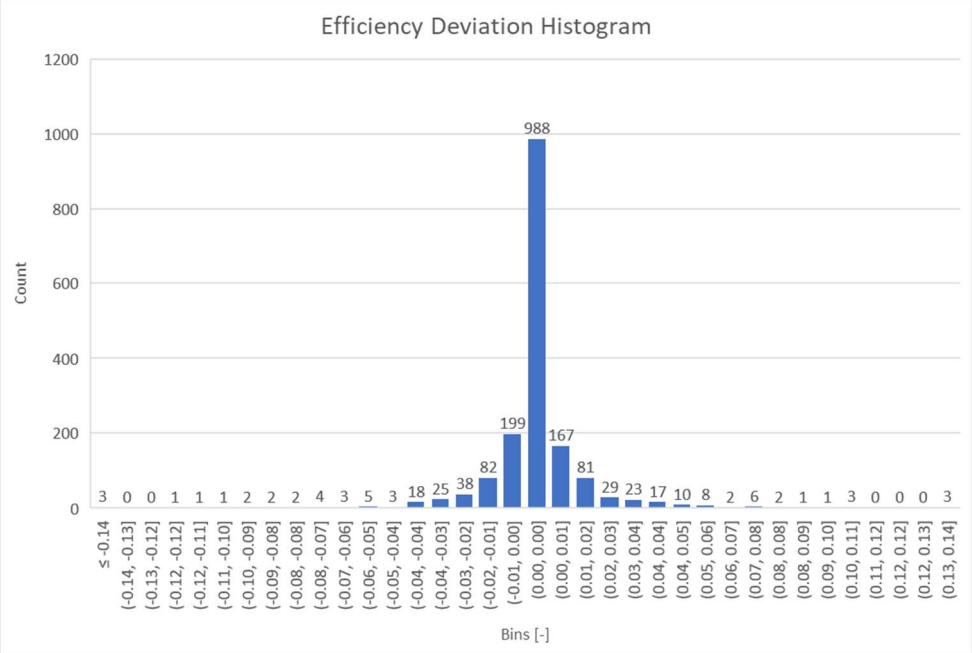

Figure 11. Histogram of Measured Efficiency Deviations.

The measurement of spread in this experiment was more uncertain than efficiency with a standard deviation in the spread deviations of 0.89-cm. Using histograms to assess the distribution fit it was found that the data fit a normal distribution fairly (Figure 12). Analyzing the uncertainty interval at a 95% level found that the uncertainty for the spread measurement was +/- 31%. The spread measurement was the most difficult to measure as surface roughness does not produce a single width especially with a complex micro-geometry.

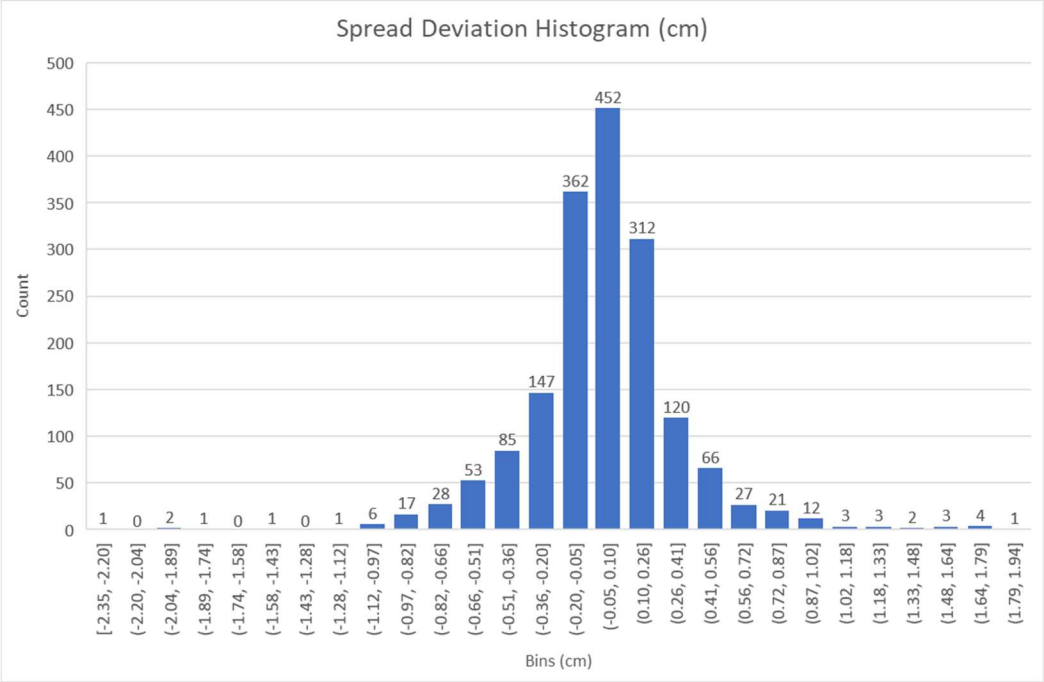

Figure 12. Histogram of Spread Measurement Deviations.

C.3 Assessment of Efficiency and Spread by model configuration

The main comparison for this study was to examine the efficiency breakdown under similar experimental conditions. In the experiment not every trial used the full four inlets and for most only 2 or 3 inlets were used based on the configuration of cross and longitudinal slopes. For this reason, breakdown of average efficiency was primary directed for the 1st inlet as inflow conditions were consistent between trails. A breakdown of averages per deck drain design based on the inflow showed (Table 7 and Table 8) that for all flow conditions that increasing the downspout size lead to an increase in efficiency. Additionally, under high flow conditions (1.59 m^3/hr.) the first inlet would be full flowing indicating it was reaching orifice control limits. As seen in the Table 7 and Table 8 changing from a round downspout to a square downspout increases the capture capacity of the inlet in this experiment. This occurs for a size increase from 20-cm to 25-cm as well. Finally, the difference between grate types was minimal but for the high flow regime the efficiency of the

downspouts performed better with exception of the 25-cm square indicating that at high flows that there is also a grate control condition as well.

Table 7. Inflow average efficiency for each design using only the most upstream inlet location data.

Inflow (m^3/hr.)	20-cm Round	20-cm Square	25-cm Round	25-cm Square
0.68	0.72 ± 0.24	0.74 ± 0.25	0.76 ± 0.26	0.74 ± 0.24
1.02	0.65 ± 0.22	0.67 ± 0.24	0.68 ± 0.24	0.68 ± 0.22
1.59	0.52 ± 0.15	0.58 ± 0.19	0.62 ± 0.22	0.63 ± 0.20

Table 8. Inflow average efficiency using all experimental data points.

Inflow (m^3/hr.)	20-cm Round	20-cm Square	25-cm Round	25-cm Square
0.68	0.75 ± 0.20	0.78 ± 0.23	0.77 ± 0.24	0.77 ± 0.22
1.02	0.61 ± 0.14	0.70 ± 0.22	0.71 ± 0.23	0.72 ± 0.23
1.59	0.44 ± 0.08	0.52 ± 0.13	0.59 ± 0.17	0.64 ± 0.20

Table 9 and Table 10 show the average efficiency breakdown for all flow regimes and deck configurations between all trials and only for the first inlet, respectively. Similar patterns are seen between the two-measure indicating that efficiency is expected to increase with increased size of the downspout. For the first inlet averages, this relationship was less clear indicating that the performance of the grate was dependent upon flow conditions as supported by Table 7. No negative impact was observed for increasing the size of the inlet or in changing the shape of the downspout. The average spread values presented in both tables indicate that while this variable is uncertain in this test that on average there is a trend of lowered spread measurements with higher efficiencies as expected based on current relationships from design literature. The vane grate is shown in Table 9 to perform better than the bar grate under a single inflow condition for the first inlet.

Table 9. Design average efficiency and spread across all inflows using only data from the single most upstream inlet location.

Inlet	Average Efficiency		Average Spread (cm)	
	Bar	Vane	Bar	Vane
20-cm Round	0.79 ± 0.15	0.79 ± 0.110	19.05 ± 7.87	19.30 ± 6.86
20-cm Square	0.81 ± 0.15	0.83 ± 0.124	18.80 ± 7.87	17.78 ± 7.37
25-cm Round	0.83 ± 0.14	0.84 ± 0.134	18.29 ± 8.13	18.03 ± 7.37
25-cm Square	0.82 ± 0.13	0.84 ± 0.126	18.29 ± 8.13	17.27 ± 7.62

Table 10. Design average efficiency and spread across all inflows using all data points.

Inlet	Average Efficiency		Average Spread (cm)	
	Bar	Vane	Bar	Vane
20-cm Round	0.62 ± 0.24	0.61 ± 0.15	28.96 ± 11.94	28.70 ± 11.68
20-cm Square	0.66 ± 0.25	0.66 ± 0.23	27.69 ± 11.18	27.43 ± 11.68
25-cm Round	0.69 ± 0.26	0.71 ± 0.24	27.69 ± 11.68	26.92 ± 11.18
25-cm Square	0.68 ± 0.23	0.71 ± 0.23	26.67 ± 11.43	26.42 ± 11.43

Figures 13 and 14 compare the average efficiency for each grate type and drain type based on the cross slope and longitudinal slope. Under a 2% cross slope (Figure 14) this experiment showed that the highest efficiency occurred at a longitudinal slope of 0.5% followed by the largest longitudinal slope of 4%. Under the 2% cross slope efficiencies at each longitudinal slope are lower compared to its counterpart at a 6% cross slope (Figure 13). For a shallow cross slope, the water was observed to spread out much more with a shallower depth resulting in less gutter flow in the inlet width. For the 6% cross slope flow channeled immediately and the water depth was significantly greater near the curb of the deck than going way from the deck. Additionally, as seen in Figure 13 and 14 the efficiency between deck drain designs is very condensed where changing the outlet has little impact on the efficiency. The largest increase in efficiency was found in Figure 14 under a 0.5% longitudinal slope with a change from the standard 20-cm design to 25-cm with a vane grate. Finally, the difference between the bar and vane grate based on slope was minimal

where the vane grate performed better at the 2% cross slope and the bar grate performed better at the 6% cross slope.

The curves shown in Figure 13 and 14 all have a similar trends where a higher efficiency is found at the smallest and largest longitudinal slopes. In the experiment at 0.5% longitudinal slope the water moved slower with less potential for splash over where it could be captured by fewer inlets, as expected. The 1% and 2% longitudinal slope showed expected trends of a decrease in efficiency most likely due to increase of water velocity creating less side flow capture. The increase at 4% longitudinal slope is likely due to the channelization of water where it could not spread out and bypass the sides of the inlet. This trend was likely due to the experimental set up as the inflow was placed in the gutter whereas at full-scale rainfall would create an even sheet flow across the surface.

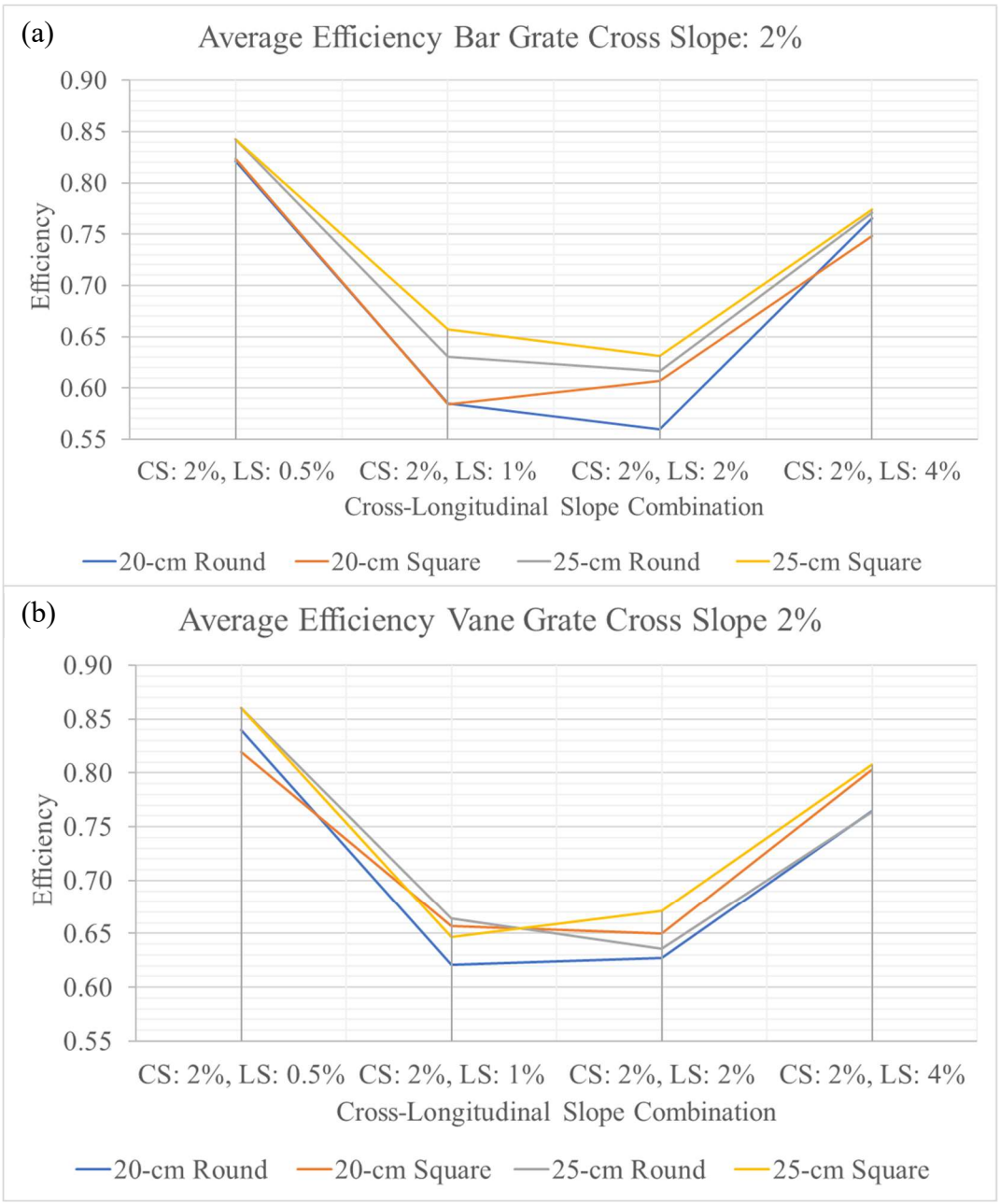

Figure 13. Average efficiency breakdown per longitudinal slope at a cross slope of 2% for (a) bar and (b) vane grates.

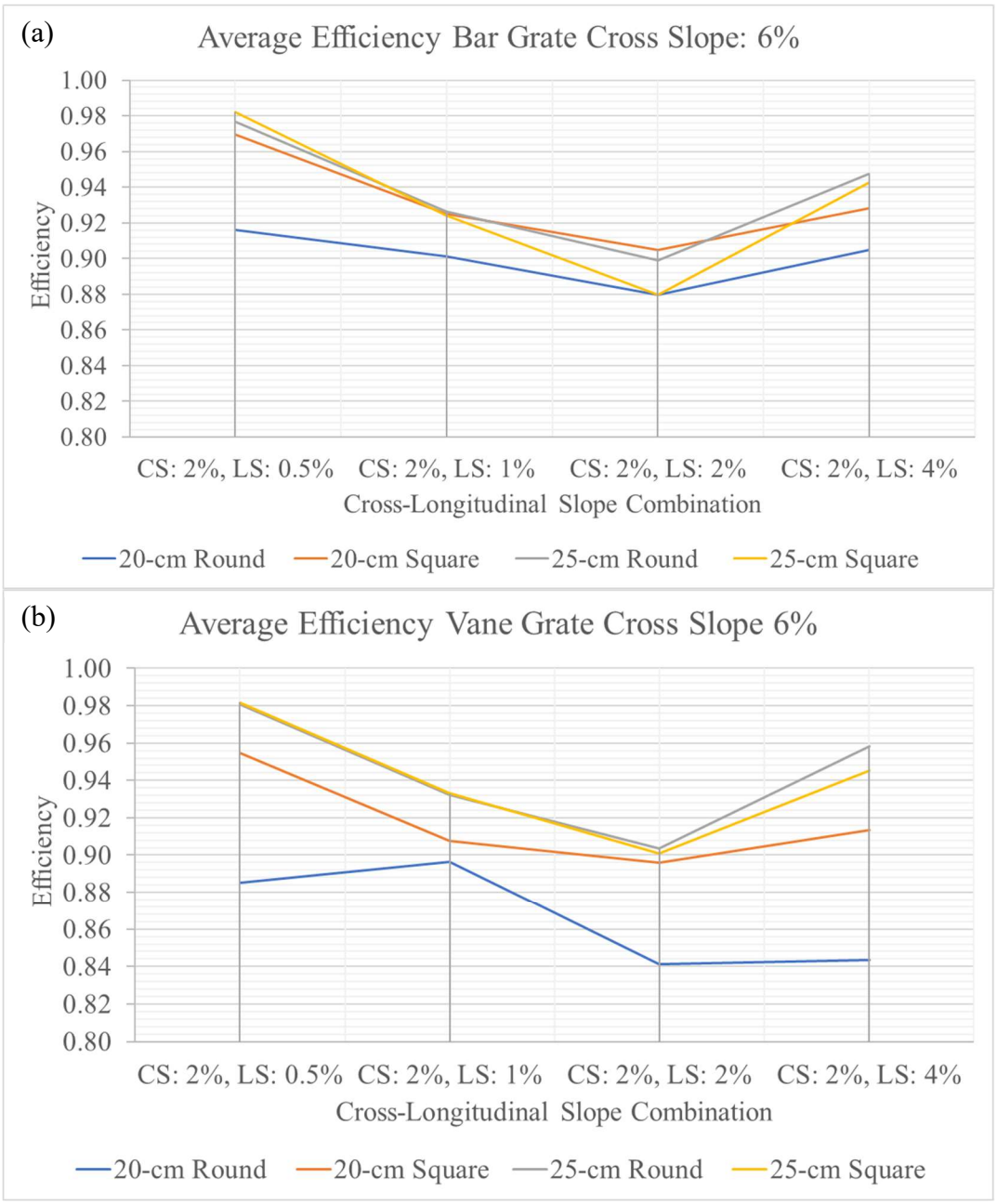

Figure 14. Average efficiency breakdown per longitudinal slope at a cross slope of 6% for (a) bar and (b) vane grates.

C.4 Assessment of Sediment Transport Data by Model Configuration

In the second set of experimental data, the main parameters analyzed were related to the erosion rate between bar and vane grates across a range of approach flow and slope combination. A Mann Whitney U signified test was performed to see if there was statistically significant difference between slope configurations and all data per vane type. At a 95% confidence level, a statistically significant difference was only found at a 6% cross slope and 4% longitudinal slope averaged across all inflows with the vane grate having better performance. Applying the standard difference of the mean test also supported these results with the same conclusion; except for comparisons based on configurations and slope. At low inflow regime with a 6% cross slope and 0.5% longitudinal slope the bar performed better with statistical significance at a 95% level. Additionally, the bar grate performed better at the high inflow regime at a 2% cross slope and 1% longitudinal slope at 95% significance level. The vane grate performed better with statistical significance at 95% level in the low flow regime with a 2% cross and longitudinal slope as well as the medium flow regime at a 6% cross slope and 2% longitudinal slope. Examining the total averages of erosion rate, it was found that the bar grate had a rate of 0.056 g/s while the vane performed slightly better with an average rate of 0.061 g/s. A further breakdown as shown in Tables 11 and 12 indicates that the only slope configuration presenting a difference in erosion rate between grates was at the 2% and 4% longitudinal slopes at a 6% cross slope resulting in the overall average different.

Table 11. Average erosion rate (g/s) across inflows based on the longitudinal slope at a 6% cross slope per grate type.

6% Cross Slope Erosion Rates (g/s)				
Grate	LS: 0.04	LS: 0.02	LS: 0.01	LS: 0.005
Bar	0.084 ± 0.071	0.046 ± 0.012	0.055 ± 0.010	0.045 ± 0.008
Vane	0.114 ± 0.062	0.066 ± 0.021	0.051 ± 0.025	0.041 ± 0.010

Table 12. average erosion rate (g/s) across inflow based on the longitudinal slope at a 2% cross slope per grate type.

2% Cross Slope Erosion Rates (g/s)				
Grate	LS: 0.04	LS: 0.02	LS: 0.01	LS: 0.005
Bar	0.063 ± 0.032	0.054 ± 0.021	0.042 ± 0.008	0.057 ± 0.017
Vane	0.064 ± 0.050	0.051 ± 0.019	0.041 ± 0.016	0.063 ± 0.032

Appendix D: Notation List

The following symbols are used in this paper:

A = area of movable surface (m^2)

C = rational runoff coefficient (dimensionless)

E = ratio of frontal and side flow to gutter flow (-)

E_o = ratio of frontal flow to total gutter flow (-)

I = design rainfall intensity (mm/hr.)

L_c = constant distance between inlets (m)

L_g = length of the inlet parallel to the flow (m)

M = total mass of sediment lost (kg)

N_m = the number of drains required (-)

Q = total gutter flow (m^3/s)

Q_c = intercepted flow (m^3/s)

$Q_{c100\%}$ = 100% of gutter flow captured (m^3/s)

Q_r = the discharge ratio (-)

R = cohesive sediment transport parameter (-)

R_f = fraction of frontal flow entering the inlet (-)

R_s = fraction of side flow (dimensionless)

S = longitudinal slope (dimensionless)

S_x = cross slope (dimensionless)

T = width of flow (m)

U = residuals between experimental and theoretical data (-)

U_e = uncertainty in residuals for each width-to-spread ratio bin defined as experimental uncertainty (-)

U_h = bin-average of residuals defined as hydraulic uncertainty (-)

V_r = the velocity ratio (-)

W = opening width of the inlet (m)

W_p = width pavement contributing to gutter flow (m)

d_{50} = median grain size (mm)

g = gravity (m/s^2)

h = hydraulic radius (m)

k_g = a constant (dimensionless)

$k_{100\%}$ = 100% capture discharge coefficient (-)

n = Manning's roughness coefficient (-)

n_r = the ratio of Manning's roughness coefficient (-)

t = measurement period (s)

u_{cr} = critical shear velocity (m/s)

u^* = shear velocity (m/s)

v = velocity of flow in the gutter (m/s)

v_o = grate specific splashover velocity (m/s)

ε = sediment entrainment rate (kg/s)

ρ = density of water (g/cm^3)

ρ_s = density of the sediment (g/cm^3)

τ_c = critical shear stress (N/m^2)

$\widetilde{\Phi}$ = shear stress parameter for cohesive sediments (-)

Appendix E: Experimental Data for Efficiency Tests

Table 13. Experimental data for efficiency tests. Flows, spread, efficiency, and WT are averages of three trial replicates

Starting Trial	Inlet Pos.	Grate Type	Shape	DS size (cm)	Cross Slope	Long Slope	Valve Reading (m^3/hr.)	Inflow (m^3/hr.)	Captured Flow (m^3/hr.)	Spread (cm)	Efficiency	WT
1	1	Vane	Round	20	0.02	0.005	0.6927	0.6267	0.5321	38.27	0.85	0.18
1	2	Vane	Round	20	0.02	0.005	0.6927	0.0943	0.0803	23.60	0.85	0.29
1	3	Vane	Round	20	0.02	0.005	0.6927	0.0142	0.0142	8.57	1.00	0.79
4	1	Vane	Round	20	0.02	0.005	1.1810	1.1764	0.7684	43.43	0.65	0.16
4	2	Vane	Round	20	0.02	0.005	1.1810	0.4025	0.2943	23.23	0.73	0.29
4	3	Vane	Round	20	0.02	0.005	1.1810	0.1107	0.1079	14.20	0.97	0.48
4	4	Vane	Round	20	0.02	0.005	1.1810	0.0033	0.0033	2.03	1.00	1.00
7	1	Vane	Round	20	0.02	0.005	1.6391	1.4601	0.7218	48.30	0.49	0.14
7	2	Vane	Round	20	0.02	0.005	1.6391	0.7382	0.4802	27.33	0.65	0.25
7	3	Vane	Round	20	0.02	0.005	1.6391	0.2581	0.2441	19.07	0.95	0.36
7	4	Vane	Round	20	0.02	0.005	1.6391	0.0139	0.0139	6.13	1.00	1.00
10	1	bar	Round	20	0.02	0.005	0.6995	0.6939	0.5800	40.03	0.84	0.17
10	2	bar	Round	20	0.02	0.005	0.6995	0.1139	0.0754	21.70	0.66	0.31
10	3	bar	Round	20	0.02	0.005	0.6995	0.0386	0.0366	9.67	0.95	0.70
10	4	bar	Round	20	0.02	0.005	0.6995	0.0020	0.0020	1.93	1.00	1.00
13	1	bar	Round	20	0.02	0.005	1.0963	1.0093	0.7530	43.50	0.75	0.16
13	2	bar	Round	20	0.02	0.005	1.0963	0.2580	0.2054	24.03	0.80	0.28
13	3	bar	Round	20	0.02	0.005	1.0963	0.0539	0.0490	12.43	0.91	0.55
13	4	bar	Round	20	0.02	0.005	1.0963	0.0053	0.0053	3.50	1.00	1.00
16	1	bar	Round	20	0.02	0.005	1.6625	1.4071	0.8532	47.77	0.61	0.14
16	2	bar	Round	20	0.02	0.005	1.6625	0.5553	0.3380	26.90	0.61	0.25
16	3	bar	Round	20	0.02	0.005	1.6625	0.2156	0.1964	20.87	0.91	0.32
16	4	bar	Round	20	0.02	0.005	1.6625	0.0184	0.0184	6.53	1.00	1.00
19	1	Vane	Sq.	20	0.02	0.005	0.7319	0.6719	0.5960	39.03	0.89	0.17
19	2	Vane	Sq.	20	0.02	0.005	0.7319	0.0758	0.0288	15.87	0.38	0.43
19	3	Vane	Sq.	20	0.02	0.005	0.7319	0.0469	0.0452	10.67	0.96	0.64
19	4	Vane	Sq.	20	0.02	0.005	0.7319	0.0017	0.0017	1.33	1.00	1.00
22	1	Vane	Sq.	20	0.02	0.005	1.0599	1.0190	0.7566	43.57	0.74	0.16
22	2	Vane	Sq.	20	0.02	0.005	1.0599	0.2632	0.1741	23.23	0.66	0.29
22	3	Vane	Sq.	20	0.02	0.005	1.0599	0.0885	0.0868	17.33	0.98	0.39
22	4	Vane	Sq.	20	0.02	0.005	1.0599	0.0018	0.0018	3.23	1.00	1.00
25	1	Vane	Sq.	20	0.02	0.005	1.6497	1.4461	0.9010	48.20	0.62	0.14
25	2	Vane	Sq.	20	0.02	0.005	1.6497	0.5486	0.3540	30.07	0.65	0.23
25	3	Vane	Sq.	20	0.02	0.005	1.6497	0.1928	0.1834	20.90	0.95	0.32
25	4	Vane	Sq.	20	0.02	0.005	1.6497	0.0094	0.0094	5.80	1.00	1.00
28	1	bar	Sq.	20	0.02	0.005	0.7120	0.6658	0.5248	35.90	0.79	0.19
28	2	bar	Sq.	20	0.02	0.005	0.7120	0.1417	0.1035	20.90	0.73	0.32
28	3	bar	Sq.	20	0.02	0.005	0.7120	0.0378	0.0378	10.60	1.00	0.64
31	1	bar	Sq.	20	0.02	0.005	1.1450	1.0948	0.7167	42.60	0.65	0.16
31	2	bar	Sq.	20	0.02	0.005	1.1450	0.3774	0.2655	25.13	0.70	0.27
31	3	bar	Sq.	20	0.02	0.005	1.1450	0.1122	0.1088	17.53	0.97	0.39
31	4	bar	Sq.	20	0.02	0.005	1.1450	0.0036	0.0036	7.30	1.00	0.93
34	1	bar	Sq.	20	0.02	0.005	1.6284	1.4662	0.8880	46.17	0.61	0.15
34	2	bar	Sq.	20	0.02	0.005	1.6284	0.5786	0.3731	28.53	0.64	0.24
34	3	bar	Sq.	20	0.02	0.005	1.6284	0.2052	0.1950	20.67	0.95	0.33
34	4	bar	Sq.	20	0.02	0.005	1.6284	0.0104	0.0104	5.63	1.00	1.00
37	1	Vane	Round	25	0.02	0.005	0.6751	0.6346	0.5670	39.77	0.89	0.17
37	2	Vane	Round	25	0.02	0.005	0.6751	0.0684	0.0459	17.70	0.67	0.38
37	3	Vane	Round	25	0.02	0.005	0.6751	0.0210	0.0210	10.13	1.00	0.67
40	1	Vane	Round	25	0.02	0.005	1.0277	0.9337	0.7166	42.07	0.77	0.16
40	2	Vane	Round	25	0.02	0.005	1.0277	0.2172	0.1621	24.93	0.75	0.27
40	3	Vane	Round	25	0.02	0.005	1.0277	0.0552	0.0512	16.47	0.93	0.41
40	4	Vane	Round	25	0.02	0.005	1.0277	0.0042	0.0042	6.70	1.00	1.00
43	1	Vane	Round	25	0.02	0.005	1.5820	1.4429	0.9490	46.17	0.66	0.15
43	2	Vane	Round	25	0.02	0.005	1.5820	0.4942	0.3366	27.57	0.68	0.25
43	3	Vane	Round	25	0.02	0.005	1.5820	0.1576	0.1506	21.33	0.96	0.32
43	4	Vane	Round	25	0.02	0.005	1.5820	0.0070	0.0070	6.43	1.00	1.00
46	1	bar	Round	25	0.02	0.005	0.6638	0.6027	0.5306	37.37	0.88	0.18
46	2	bar	Round	25	0.02	0.005	0.6638	0.0726	0.0546	20.37	0.75	0.33
46	3	bar	Round	25	0.02	0.005	0.6638	0.0174	0.0174	12.90	1.00	0.53
49	1	bar	Round	25	0.02	0.005	1.1145	1.0342	0.7365	41.80	0.71	0.16
49	2	bar	Round	25	0.02	0.005	1.1145	0.2968	0.1922	24.20	0.65	0.28
49	3	bar	Round	25	0.02	0.005	1.1145	0.1085	0.1004	17.50	0.93	0.39
49	4	bar	Round	25	0.02	0.005	1.1145	0.0085	0.0085	6.37	1.00	1.00
52	1	bar	Round	25	0.02	0.005	1.6088	1.3319	0.8541	44.37	0.64	0.15

52	2	bar	Round	25	0.02	0.005	1.6088	0.4806	0.2558	28.23	0.53	0.24
52	3	bar	Round	25	0.02	0.005	1.6088	0.2223	0.2079	18.17	0.94	0.37
52	4	bar	Round	25	0.02	0.005	1.6088	0.0143	0.0143	6.47	1.00	1.00
55	1	Vane	Sq.	25	0.02	0.005	0.6651	0.6015	0.5155	37.77	0.86	0.18
55	2	Vane	Sq.	25	0.02	0.005	0.6651	0.0833	0.0644	18.83	0.77	0.36
55	3	Vane	Sq.	25	0.02	0.005	0.6651	0.0222	0.0222	10.03	1.00	0.68
58	1	Vane	Sq.	25	0.02	0.005	1.0386	0.8772	0.6582	40.03	0.75	0.17
58	2	Vane	Sq.	25	0.02	0.005	1.0386	0.2190	0.1579	21.43	0.72	0.32
58	3	Vane	Sq.	25	0.02	0.005	1.0386	0.0611	0.0611	14.43	1.00	0.47
61	1	Vane	Sq.	25	0.02	0.005	1.5960	1.4169	0.9083	44.27	0.64	0.15
61	2	Vane	Sq.	25	0.02	0.005	1.5960	0.5085	0.3221	24.87	0.63	0.27
61	3	Vane	Sq.	25	0.02	0.005	1.5960	0.1862	0.1715	19.53	0.92	0.35
61	4	Vane	Sq.	25	0.02	0.005	1.5960	0.0150	0.0150	6.77	1.00	1.00
64	1	bar	Sq.	25	0.02	0.005	0.6863	0.6135	0.4440	37.63	0.72	0.18
64	2	bar	Sq.	25	0.02	0.005	0.6863	0.1695	0.1129	21.33	0.67	0.32
64	3	bar	Sq.	25	0.02	0.005	0.6863	0.0566	0.0566	17.83	1.00	0.38
67	1	bar	Sq.	25	0.02	0.005	1.0459	0.9458	0.6244	39.53	0.66	0.17
67	2	bar	Sq.	25	0.02	0.005	1.0459	0.3215	0.2221	22.13	0.69	0.31
67	3	bar	Sq.	25	0.02	0.005	1.0459	0.1001	0.1001	19.43	1.00	0.35
70	1	bar	Sq.	25	0.02	0.005	1.5911	1.3918	0.8499	45.37	0.61	0.15
70	2	bar	Sq.	25	0.02	0.005	1.5911	0.5403	0.3681	25.40	0.68	0.27
70	3	bar	Sq.	25	0.02	0.005	1.5911	0.1748	0.1540	21.30	0.88	0.32
70	4	bar	Sq.	25	0.02	0.005	1.5911	0.0205	0.0205	7.27	1.00	0.93
73	1	Vane	Round	20	0.06	0.005	0.7067	0.5763	0.5702	18.10	0.99	0.37
73	2	Vane	Round	20	0.06	0.005	0.7067	0.0057	0.0057	5.13	1.00	1.00
76	1	Vane	Round	20	0.06	0.005	1.1155	1.0823	0.7780	21.13	0.72	0.32
76	2	Vane	Round	20	0.06	0.005	1.1155	0.3110	0.2915	12.37	0.94	0.55
76	3	Vane	Round	20	0.06	0.005	1.1155	0.0195	0.0195	7.10	1.00	0.95
79	1	Vane	Round	20	0.06	0.005	1.6342	1.4331	0.8100	22.40	0.57	0.30
79	2	Vane	Round	20	0.06	0.005	1.6342	0.6236	0.5721	14.77	0.92	0.46
79	3	Vane	Round	20	0.06	0.005	1.6342	0.0516	0.0516	9.80	1.00	0.69
82	1	bar	Round	20	0.06	0.005	0.7028	0.6339	0.6234	16.90	0.98	0.40
82	2	bar	Round	20	0.06	0.005	0.7028	0.0104	0.0104	5.13	1.00	1.00
85	1	bar	Round	20	0.06	0.005	1.0652	0.9156	0.8407	19.63	0.92	0.35
85	2	bar	Round	20	0.06	0.005	1.0652	0.0748	0.0733	8.40	0.98	0.81
85	3	bar	Round	20	0.06	0.005	1.0652	0.0023	0.0015	4.00	0.67	1.00
88	1	bar	Round	20	0.06	0.005	1.6094	1.4189	0.8429	22.80	0.59	0.30
88	2	bar	Round	20	0.06	0.005	1.6094	0.5758	0.5345	13.73	0.93	0.49
88	3	bar	Round	20	0.06	0.005	1.6094	0.0415	0.0415	9.10	1.00	0.75
91	1	Vane	Sq.	20	0.06	0.005	0.7170	0.6419	0.6373	17.43	0.99	0.39
91	2	Vane	Sq.	20	0.06	0.005	0.7170	0.0045	0.0045	3.10	1.00	1.00
94	1	Vane	Sq.	20	0.06	0.005	1.0492	0.9376	0.8940	19.23	0.95	0.35
94	2	Vane	Sq.	20	0.06	0.005	1.0492	0.0438	0.0438	7.00	1.00	0.97
97	1	Vane	Sq.	20	0.06	0.005	1.6125	1.4199	0.9364	22.73	0.66	0.30
97	2	Vane	Sq.	20	0.06	0.005	1.6125	0.4831	0.4787	12.93	0.99	0.52
97	3	Vane	Sq.	20	0.06	0.005	1.6125	0.0044	0.0044	7.33	1.00	0.92
100	1	bar	Sq.	20	0.06	0.005	0.6952	0.6143	0.6125	16.70	1.00	0.41
100	2	bar	Sq.	20	0.06	0.005	0.6952	0.0018	0.0018	2.67	1.00	1.00
103	1	bar	Sq.	20	0.06	0.005	1.1411	0.9082	0.8797	20.17	0.97	0.34
103	2	bar	Sq.	20	0.06	0.005	1.1411	0.0311	0.0311	5.07	1.00	1.00
106	1	bar	Sq.	20	0.06	0.005	1.5897	1.4196	1.1411	22.73	0.80	0.30
106	2	bar	Sq.	20	0.06	0.005	1.5897	0.2758	0.2680	10.07	0.97	0.67
106	3	bar	Sq.	20	0.06	0.005	1.5897	0.0077	0.0077	6.70	1.00	1.00
109	1	Vane	Round	25	0.06	0.005	0.7429	0.6701	0.6667	15.97	0.99	0.42
109	2	Vane	Round	25	0.06	0.005	0.7429	0.0035	0.0035	1.90	1.00	1.00
112	1	Vane	Round	25	0.06	0.005	1.1568	1.0414	1.0011	19.97	0.96	0.34
112	2	Vane	Round	25	0.06	0.005	1.1568	0.0415	0.0415	6.37	1.00	1.00
115	1	Vane	Round	25	0.06	0.005	1.5922	1.4518	1.1716	20.57	0.81	0.33
115	2	Vane	Round	25	0.06	0.005	1.5922	0.2801	0.2744	10.00	0.98	0.68
115	3	Vane	Round	25	0.06	0.005	1.5922	0.0058	0.0058	7.20	1.00	0.94
118	1	bar	Round	25	0.06	0.005	0.7300	0.6908	0.6829	17.33	0.99	0.39
118	2	bar	Round	25	0.06	0.005	0.7300	0.0080	0.0080	4.27	1.00	1.00
121	1	bar	Round	25	0.06	0.005	1.1584	1.0606	1.0113	19.63	0.95	0.35
121	2	bar	Round	25	0.06	0.005	1.1584	0.0498	0.0498	7.60	1.00	0.89
124	1	bar	Round	25	0.06	0.005	1.6392	1.4529	1.3058	22.27	0.90	0.30
124	2	bar	Round	25	0.06	0.005	1.6392	0.1471	0.1439	8.87	0.98	0.76
124	3	bar	Round	25	0.06	0.005	1.6392	0.0032	0.0032	4.87	1.00	1.00
127	1	Vane	Sq.	25	0.06	0.005	0.6701	0.6150	0.6105	16.93	0.99	0.40
127	2	Vane	Sq.	25	0.06	0.005	0.6701	0.0044	0.0044	2.87	1.00	1.00
130	1	Vane	Sq.	25	0.06	0.005	1.0669	0.9486	0.9249	19.47	0.98	0.35
130	2	Vane	Sq.	25	0.06	0.005	1.0669	0.0236	0.0236	5.77	1.00	1.00
133	1	Vane	Sq.	25	0.06	0.005	1.5769	1.3826	1.2379	20.18	0.90	0.34
133	2	Vane	Sq.	25	0.06	0.005	1.5769	0.1445	0.1429	8.47	0.99	0.80
133	3	Vane	Sq.	25	0.06	0.005	1.5769	0.0016	0.0016	2.23	1.00	1.00
136	1	bar	Sq.	25	0.06	0.005	0.7200	0.6355	0.6313	16.77	0.99	0.40

136	2	bar	Sq.	25	0.06	0.005	0.7200	0.0043	0.0043	4.67	1.00	1.00
139	1	bar	Sq.	25	0.06	0.005	1.0731	0.9276	0.9056	18.87	0.98	0.36
139	2	bar	Sq.	25	0.06	0.005	1.0731	0.0220	0.0220	5.87	1.00	1.00
142	1	bar	Sq.	25	0.06	0.005	1.6273	1.4539	1.3089	21.53	0.90	0.31
142	2	bar	Sq.	25	0.06	0.005	1.6273	0.1450	0.1428	8.53	0.98	0.79
142	3	bar	Sq.	25	0.06	0.005	1.6273	0.0022	0.0022	3.17	1.00	1.00
145	1	Vane	Round	20	0.02	0.01	0.6870	0.6111	0.3353	38.93	0.55	0.17
145	2	Vane	Round	20	0.02	0.01	0.6870	0.2756	0.1228	33.53	0.45	0.20
145	3	Vane	Round	20	0.02	0.01	0.6870	0.1534	0.0909	26.47	0.59	0.26
145	4	Vane	Round	20	0.02	0.01	0.6870	0.0620	0.0620	9.70	1.00	0.70
148	1	Vane	Round	20	0.02	0.01	1.0842	0.9820	0.4442	40.83	0.45	0.17
148	2	Vane	Round	20	0.02	0.01	1.0842	0.5395	0.2342	34.73	0.43	0.20
148	3	Vane	Round	20	0.02	0.01	1.0842	0.3042	0.1817	31.00	0.60	0.22
148	4	Vane	Round	20	0.02	0.01	1.0842	0.1221	0.1221	12.73	1.00	0.53
151	1	Vane	Round	20	0.02	0.01	1.5973	1.4220	0.5480	43.83	0.39	0.15
151	2	Vane	Round	20	0.02	0.01	1.5973	0.8746	0.3396	37.37	0.39	0.18
151	3	Vane	Round	20	0.02	0.01	1.5973	0.5346	0.2452	34.10	0.46	0.20
151	4	Vane	Round	20	0.02	0.01	1.5973	0.2894	0.2894	15.33	1.00	0.44
154	1	bar	Round	20	0.02	0.01	0.7390	0.6329	0.2710	37.10	0.43	0.18
154	2	bar	Round	20	0.02	0.01	0.7390	0.3623	0.1413	33.63	0.39	0.20
154	3	bar	Round	20	0.02	0.01	0.7390	0.2228	0.1420	28.30	0.64	0.24
154	4	bar	Round	20	0.02	0.01	0.7390	0.0787	0.0787	11.20	1.00	0.61
157	1	bar	Round	20	0.02	0.01	1.0642	0.9313	0.3686	39.80	0.40	0.17
157	2	bar	Round	20	0.02	0.01	1.0642	0.5635	0.2223	36.10	0.39	0.19
157	3	bar	Round	20	0.02	0.01	1.0642	0.3403	0.2270	32.23	0.67	0.21
157	4	bar	Round	20	0.02	0.01	1.0642	0.1138	0.1138	13.50	1.00	0.50
160	1	bar	Round	20	0.02	0.01	1.6493	1.4682	0.5032	44.73	0.34	0.15
160	2	bar	Round	20	0.02	0.01	1.6493	0.9649	0.3571	38.80	0.37	0.17
160	3	bar	Round	20	0.02	0.01	1.6493	0.6078	0.3117	36.17	0.51	0.19
160	4	bar	Round	20	0.02	0.01	1.6493	0.2961	0.2961	14.67	1.00	0.46
163	1	Vane	Sq.	20	0.02	0.01	0.6460	0.6048	0.3331	36.03	0.55	0.19
163	2	Vane	Sq.	20	0.02	0.01	0.6460	0.2714	0.1148	29.73	0.42	0.23
163	3	Vane	Sq.	20	0.02	0.01	0.6460	0.1566	0.1303	23.70	0.83	0.29
163	4	Vane	Sq.	20	0.02	0.01	0.6460	0.0264	0.0264	8.33	1.00	0.81
166	1	Vane	Sq.	20	0.02	0.01	1.0078	0.8932	0.4259	38.63	0.48	0.18
166	2	Vane	Sq.	20	0.02	0.01	1.0078	0.4673	0.1763	33.90	0.38	0.20
166	3	Vane	Sq.	20	0.02	0.01	1.0078	0.2911	0.2528	31.20	0.87	0.22
166	4	Vane	Sq.	20	0.02	0.01	1.0078	0.0383	0.0383	11.03	1.00	0.61
169	1	Vane	Sq.	20	0.02	0.01	1.6518	1.4221	0.5585	43.07	0.39	0.16
169	2	Vane	Sq.	20	0.02	0.01	1.6518	0.8628	0.3125	39.37	0.36	0.17
169	3	Vane	Sq.	20	0.02	0.01	1.6518	0.5506	0.3312	33.53	0.60	0.20
169	4	Vane	Sq.	20	0.02	0.01	1.6518	0.2200	0.2200	13.60	1.00	0.50
172	1	bar	Sq.	20	0.02	0.01	0.6990	0.6223	0.3079	33.70	0.49	0.20
172	2	bar	Sq.	20	0.02	0.01	0.6990	0.3134	0.1148	32.03	0.37	0.21
172	3	bar	Sq.	20	0.02	0.01	0.6990	0.1981	0.1259	31.20	0.64	0.22
172	4	bar	Sq.	20	0.02	0.01	0.6990	0.0732	0.0732	10.30	1.00	0.66
175	1	bar	Sq.	20	0.02	0.01	1.0478	0.9602	0.3964	40.90	0.41	0.17
175	2	bar	Sq.	20	0.02	0.01	1.0478	0.5637	0.1720	35.70	0.31	0.19
175	3	bar	Sq.	20	0.02	0.01	1.0478	0.3924	0.2208	32.97	0.56	0.21
175	4	bar	Sq.	20	0.02	0.01	1.0478	0.1720	0.1720	12.40	1.00	0.55
178	1	bar	Sq.	20	0.02	0.01	1.4717	1.3621	0.5264	43.10	0.39	0.16
178	2	bar	Sq.	20	0.02	0.01	1.4717	0.8352	0.2983	40.10	0.36	0.17
178	3	bar	Sq.	20	0.02	0.01	1.4717	0.5373	0.2645	36.60	0.49	0.19
178	4	bar	Sq.	20	0.02	0.01	1.4717	0.2731	0.2731	13.17	1.00	0.51
181	1	Vane	Round	25	0.02	0.01	0.6599	0.5638	0.3056	36.07	0.54	0.19
181	2	Vane	Round	25	0.02	0.01	0.6599	0.2537	0.0993	31.73	0.39	0.21
181	3	Vane	Round	25	0.02	0.01	0.6599	0.1567	0.1313	26.80	0.84	0.25
181	4	Vane	Round	25	0.02	0.01	0.6599	0.0255	0.0255	9.77	1.00	0.69
184	1	Vane	Round	25	0.02	0.01	1.0532	0.9000	0.4494	38.93	0.50	0.17
184	2	Vane	Round	25	0.02	0.01	1.0532	0.4491	0.1838	34.07	0.41	0.20
184	3	Vane	Round	25	0.02	0.01	1.0532	0.2681	0.2004	34.40	0.75	0.20
184	4	Vane	Round	25	0.02	0.01	1.0532	0.0669	0.0669	11.07	1.00	0.61
187	1	Vane	Round	25	0.02	0.01	1.6575	1.4345	0.6108	43.80	0.43	0.15
187	2	Vane	Round	25	0.02	0.01	1.6575	0.8234	0.2991	39.57	0.36	0.17
187	3	Vane	Round	25	0.02	0.01	1.6575	0.5245	0.2936	37.13	0.56	0.18
187	4	Vane	Round	25	0.02	0.01	1.6575	0.2311	0.2311	14.37	1.00	0.47
190	1	bar	Round	25	0.02	0.01	0.6703	0.6120	0.3163	36.33	0.52	0.19
190	2	bar	Round	25	0.02	0.01	0.6703	0.2953	0.1220	33.13	0.41	0.20
190	3	bar	Round	25	0.02	0.01	0.6703	0.1736	0.1384	30.37	0.80	0.22
190	4	bar	Round	25	0.02	0.01	0.6703	0.0356	0.0356	10.20	1.00	0.66
193	1	bar	Round	25	0.02	0.01	1.0235	0.9240	0.4183	39.90	0.45	0.17
193	2	bar	Round	25	0.02	0.01	1.0235	0.5058	0.1855	36.17	0.37	0.19
193	3	bar	Round	25	0.02	0.01	1.0235	0.3202	0.2618	34.00	0.82	0.20
193	4	bar	Round	25	0.02	0.01	1.0235	0.0586	0.0586	11.40	1.00	0.59
196	1	bar	Round	25	0.02	0.01	1.5939	1.4169	0.5682	43.53	0.40	0.16

196	2	bar	Round	25	0.02	0.01	1.5939	0.8494	0.2749	38.47	0.32	0.18
196	3	bar	Round	25	0.02	0.01	1.5939	0.5741	0.3404	36.47	0.59	0.19
196	4	bar	Round	25	0.02	0.01	1.5939	0.2338	0.2338	14.93	1.00	0.45
199	1	Vane	Sq.	25	0.02	0.01	0.6805	0.6112	0.3405	36.60	0.56	0.19
199	2	Vane	Sq.	25	0.02	0.01	0.6805	0.2734	0.1207	29.93	0.44	0.23
199	3	Vane	Sq.	25	0.02	0.01	0.6805	0.1507	0.1186	28.10	0.79	0.24
199	4	Vane	Sq.	25	0.02	0.01	0.6805	0.0325	0.0325	8.67	1.00	0.78
202	1	Vane	Sq.	25	0.02	0.01	1.0362	0.8907	0.4398	40.00	0.49	0.17
202	2	Vane	Sq.	25	0.02	0.01	1.0362	0.4513	0.1646	34.77	0.36	0.20
202	3	Vane	Sq.	25	0.02	0.01	1.0362	0.2869	0.2243	30.77	0.78	0.22
202	4	Vane	Sq.	25	0.02	0.01	1.0362	0.0623	0.0623	12.03	1.00	0.56
205	1	Vane	Sq.	25	0.02	0.01	1.6051	1.4077	0.5907	44.37	0.42	0.15
205	2	Vane	Sq.	25	0.02	0.01	1.6051	0.8170	0.2830	37.10	0.35	0.18
205	3	Vane	Sq.	25	0.02	0.01	1.6051	0.5340	0.3041	35.00	0.57	0.19
205	4	Vane	Sq.	25	0.02	0.01	1.6051	0.2300	0.2300	15.03	1.00	0.45
208	1	bar	Sq.	25	0.02	0.01	0.6811	0.6092	0.3602	37.10	0.59	0.18
208	2	bar	Sq.	25	0.02	0.01	0.6811	0.2482	0.1031	32.13	0.42	0.21
208	3	bar	Sq.	25	0.02	0.01	0.6811	0.1443	0.1154	28.13	0.80	0.24
208	4	bar	Sq.	25	0.02	0.01	0.6811	0.0305	0.0305	9.93	1.00	0.68
211	1	bar	Sq.	25	0.02	0.01	1.0679	0.9231	0.4898	40.20	0.53	0.17
211	2	bar	Sq.	25	0.02	0.01	1.0679	0.4330	0.1569	35.50	0.36	0.19
211	3	bar	Sq.	25	0.02	0.01	1.0679	0.2755	0.2064	31.57	0.75	0.21
211	4	bar	Sq.	25	0.02	0.01	1.0679	0.0690	0.0690	11.87	1.00	0.57
214	1	bar	Sq.	25	0.02	0.01	1.6535	1.4337	0.6840	42.63	0.48	0.16
214	2	bar	Sq.	25	0.02	0.01	1.6535	0.7484	0.2417	36.67	0.32	0.18
214	3	bar	Sq.	25	0.02	0.01	1.6535	0.5049	0.3215	32.90	0.64	0.21
214	4	bar	Sq.	25	0.02	0.01	1.6535	0.1863	0.1863	15.40	1.00	0.44
217	1	Vane	Round	20	0.06	0.01	0.6842	0.6213	0.5548	19.10	0.89	0.35
217	2	Vane	Round	20	0.06	0.01	0.6842	0.0666	0.0666	9.80	1.00	0.69
220	1	Vane	Round	20	0.06	0.01	1.0488	0.9120	0.6544	19.97	0.72	0.34
220	2	Vane	Round	20	0.06	0.01	1.0488	0.2585	0.2511	12.87	0.97	0.53
220	3	Vane	Round	20	0.06	0.01	1.0488	0.0073	0.0073	9.27	1.00	0.73
223	1	Vane	Round	20	0.06	0.01	1.6300	1.3927	0.6969	21.77	0.50	0.31
223	2	Vane	Round	20	0.06	0.01	1.6300	0.6976	0.5617	18.60	0.81	0.36
223	3	Vane	Round	20	0.06	0.01	1.6300	0.1349	0.1333	12.83	0.99	0.53
223	4	Vane	Round	20	0.06	0.01	1.6300	0.0017	0.0017	3.00	1.00	1.00
226	1	bar	Round	20	0.06	0.01	0.6870	0.6021	0.5315	17.87	0.88	0.38
226	2	bar	Round	20	0.06	0.01	0.6870	0.0704	0.0704	9.20	1.00	0.74
229	1	bar	Round	20	0.06	0.01	1.0434	0.9432	0.8033	19.90	0.85	0.34
229	2	bar	Round	20	0.06	0.01	1.0434	0.1396	0.1359	11.20	0.97	0.61
229	3	bar	Round	20	0.06	0.01	1.0434	0.0036	0.0036	6.07	1.00	1.00
232	1	bar	Round	20	0.06	0.01	1.4756	1.3390	0.9318	21.80	0.70	0.31
232	2	bar	Round	20	0.06	0.01	1.4756	0.4065	0.3605	14.20	0.89	0.48
232	3	bar	Round	20	0.06	0.01	1.4756	0.0462	0.0462	10.63	1.00	0.64
235	1	Vane	Sq.	20	0.06	0.01	0.6884	0.6178	0.5561	15.00	0.90	0.45
235	2	Vane	Sq.	20	0.06	0.01	0.6884	0.0617	0.0617	7.30	1.00	0.93
238	1	Vane	Sq.	20	0.06	0.01	1.0018	0.9119	0.7772	18.70	0.85	0.36
238	2	Vane	Sq.	20	0.06	0.01	1.0018	0.1347	0.1347	9.23	1.00	0.73
241	1	Vane	Sq.	20	0.06	0.01	1.6392	1.3594	0.8527	22.27	0.63	0.30
241	2	Vane	Sq.	20	0.06	0.01	1.6392	0.5068	0.4631	14.20	0.91	0.48
241	3	Vane	Sq.	20	0.06	0.01	1.6392	0.0437	0.0437	9.20	1.00	0.74
244	1	bar	Sq.	20	0.06	0.01	0.6734	0.5909	0.5203	15.73	0.88	0.43
244	2	bar	Sq.	20	0.06	0.01	0.6734	0.0706	0.0706	9.43	1.00	0.72
247	1	bar	Sq.	20	0.06	0.01	0.9939	0.8940	0.7503	18.27	0.84	0.37
247	2	bar	Sq.	20	0.06	0.01	0.9939	0.1435	0.1435	10.87	1.00	0.62
250	1	bar	Sq.	20	0.06	0.01	1.5978	1.3830	1.0627	22.00	0.77	0.31
250	2	bar	Sq.	20	0.06	0.01	1.5978	0.3203	0.3136	12.53	0.98	0.54
250	3	bar	Sq.	20	0.06	0.01	1.5978	0.0067	0.0067	7.73	1.00	0.88
253	1	Vane	Round	25	0.06	0.01	0.6767	0.6060	0.5593	15.07	0.92	0.45
253	2	Vane	Round	25	0.06	0.01	0.6767	0.0467	0.0467	6.83	1.00	0.99
256	1	Vane	Round	25	0.06	0.01	1.0268	0.9037	0.7815	17.73	0.86	0.38
256	2	Vane	Round	25	0.06	0.01	1.0268	0.1223	0.1223	8.80	1.00	0.77
259	1	Vane	Round	25	0.06	0.01	1.6682	1.3833	1.0286	21.83	0.74	0.31
259	2	Vane	Round	25	0.06	0.01	1.6682	0.3547	0.3474	13.60	0.98	0.50
259	3	Vane	Round	25	0.06	0.01	1.6682	0.0073	0.0073	8.50	1.00	0.80
262	1	bar	Round	25	0.06	0.01	0.6641	0.5877	0.5383	14.90	0.92	0.46
262	2	bar	Round	25	0.06	0.01	0.6641	0.0494	0.0494	8.10	1.00	0.84
265	1	bar	Round	25	0.06	0.01	1.0482	0.8957	0.7726	17.40	0.86	0.39
265	2	bar	Round	25	0.06	0.01	1.0482	0.1232	0.1232	9.80	1.00	0.69
268	1	bar	Round	25	0.06	0.01	1.6228	1.3922	1.1095	19.20	0.80	0.35
268	2	bar	Round	25	0.06	0.01	1.6228	0.2823	0.2802	11.90	0.99	0.57
271	1	Vane	Sq.	25	0.06	0.01	0.6592	0.5798	0.5414	14.23	0.93	0.48
271	2	Vane	Sq.	25	0.06	0.01	0.6592	0.0385	0.0385	6.53	1.00	1.00
274	1	Vane	Sq.	25	0.06	0.01	1.0448	0.9039	0.7859	16.83	0.87	0.40
274	2	Vane	Sq.	25	0.06	0.01	1.0448	0.1180	0.1180	7.20	1.00	0.94

277	1	Vane	Sq.	25	0.06	0.01	1.5800	1.3088	1.0406	19.30	0.80	0.35
277	2	Vane	Sq.	25	0.06	0.01	1.5800	0.2680	0.2680	10.23	1.00	0.66
280	1	bar	Sq.	25	0.06	0.01	0.6562	0.5754	0.5265	13.90	0.92	0.49
280	2	bar	Sq.	25	0.06	0.01	0.6562	0.0491	0.0491	6.00	1.00	1.00
283	1	bar	Sq.	25	0.06	0.01	1.0427	0.8815	0.7514	16.33	0.85	0.42
283	2	bar	Sq.	25	0.06	0.01	1.0427	0.1300	0.1300	7.63	1.00	0.89
286	1	bar	Sq.	25	0.06	0.01	1.5343	1.3334	1.0373	19.73	0.78	0.34
286	2	bar	Sq.	25	0.06	0.01	1.5343	0.2961	0.2961	9.87	1.00	0.69
289	1	Vane	Round	20	0.02	0.02	0.6400	0.5280	0.1742	38.33	0.33	0.18
289	2	Vane	Round	20	0.02	0.02	0.6400	0.3557	0.1963	28.67	0.55	0.24
289	3	Vane	Round	20	0.02	0.02	0.6400	0.1571	0.1190	23.80	0.76	0.28
289	4	Vane	Round	20	0.02	0.02	0.6400	0.0391	0.0391	9.73	1.00	0.70
292	1	Vane	Round	20	0.02	0.02	1.0079	0.8224	0.2557	42.33	0.31	0.16
292	2	Vane	Round	20	0.02	0.02	1.0079	0.5673	0.2866	32.57	0.51	0.21
292	3	Vane	Round	20	0.02	0.02	1.0079	0.2804	0.1939	27.97	0.69	0.24
292	4	Vane	Round	20	0.02	0.02	1.0079	0.0865	0.0865	10.20	1.00	0.66
295	1	Vane	Round	20	0.02	0.02	1.6859	1.3197	0.3678	47.87	0.28	0.14
295	2	Vane	Round	20	0.02	0.02	1.6859	0.9520	0.4059	38.33	0.43	0.18
295	3	Vane	Round	20	0.02	0.02	1.6859	0.5452	0.2975	30.40	0.55	0.22
295	4	Vane	Round	20	0.02	0.02	1.6859	0.2477	0.2477	15.00	1.00	0.45
298	1	bar	Round	20	0.02	0.02	0.6788	0.5463	0.1390	38.17	0.25	0.18
298	2	bar	Round	20	0.02	0.02	0.6788	0.4075	0.2135	31.77	0.52	0.21
298	3	bar	Round	20	0.02	0.02	0.6788	0.1940	0.1287	24.40	0.66	0.28
298	4	bar	Round	20	0.02	0.02	0.6788	0.0652	0.0652	9.87	1.00	0.69
301	1	bar	Round	20	0.02	0.02	1.0286	0.8447	0.1930	44.13	0.23	0.15
301	2	bar	Round	20	0.02	0.02	1.0286	0.6518	0.2877	35.40	0.44	0.19
301	3	bar	Round	20	0.02	0.02	1.0286	0.3645	0.1866	28.63	0.51	0.24
301	4	bar	Round	20	0.02	0.02	1.0286	0.1777	0.1777	12.50	1.00	0.54
304	1	bar	Round	20	0.02	0.02	1.5320	1.3593	0.2815	47.63	0.21	0.14
304	2	bar	Round	20	0.02	0.02	1.5320	1.0778	0.4529	37.50	0.42	0.18
304	3	bar	Round	20	0.02	0.02	1.5320	0.6250	0.2577	31.03	0.41	0.22
304	4	bar	Round	20	0.02	0.02	1.5320	0.3673	0.3673	15.57	1.00	0.44
307	1	Vane	Sq.	20	0.02	0.02	0.6423	0.5540	0.1576	36.23	0.28	0.19
307	2	Vane	Sq.	20	0.02	0.02	0.6423	0.3978	0.2650	30.60	0.67	0.22
307	3	Vane	Sq.	20	0.02	0.02	0.6423	0.1325	0.1235	21.60	0.93	0.31
307	4	Vane	Sq.	20	0.02	0.02	0.6423	0.0090	0.0090	6.43	1.00	1.00
310	1	Vane	Sq.	20	0.02	0.02	0.9970	0.8871	0.2319	38.77	0.26	0.17
310	2	Vane	Sq.	20	0.02	0.02	0.9970	0.6553	0.3731	34.20	0.57	0.20
310	3	Vane	Sq.	20	0.02	0.02	0.9970	0.2822	0.2289	26.70	0.81	0.25
310	4	Vane	Sq.	20	0.02	0.02	0.9970	0.0535	0.0535	9.27	1.00	0.73
313	1	Vane	Sq.	20	0.02	0.02	1.5753	1.4138	0.3324	45.10	0.24	0.15
313	2	Vane	Sq.	20	0.02	0.02	1.5753	1.0814	0.5290	36.90	0.49	0.18
313	3	Vane	Sq.	20	0.02	0.02	1.5753	0.5524	0.3027	28.13	0.55	0.24
313	4	Vane	Sq.	20	0.02	0.02	1.5753	0.2498	0.2498	13.80	1.00	0.49
316	1	bar	Sq.	20	0.02	0.02	0.6639	0.5885	0.1289	37.17	0.22	0.18
316	2	bar	Sq.	20	0.02	0.02	0.6639	0.4597	0.2612	30.67	0.57	0.22
316	3	bar	Sq.	20	0.02	0.02	0.6639	0.1985	0.1802	22.60	0.91	0.30
316	4	bar	Sq.	20	0.02	0.02	0.6639	0.0183	0.0183	8.50	1.00	0.80
319	1	bar	Sq.	20	0.02	0.02	1.0260	0.9278	0.1950	39.33	0.21	0.17
319	2	bar	Sq.	20	0.02	0.02	1.0260	0.7329	0.3625	35.20	0.49	0.19
319	3	bar	Sq.	20	0.02	0.02	1.0260	0.3703	0.2667	28.50	0.72	0.24
319	4	bar	Sq.	20	0.02	0.02	1.0260	0.1037	0.1037	11.57	1.00	0.59
322	1	bar	Sq.	20	0.02	0.02	1.6234	1.4290	0.2890	43.13	0.20	0.16
322	2	bar	Sq.	20	0.02	0.02	1.6234	1.1400	0.5186	38.63	0.45	0.18
322	3	bar	Sq.	20	0.02	0.02	1.6234	0.6213	0.3155	30.97	0.51	0.22
322	4	bar	Sq.	20	0.02	0.02	1.6234	0.3059	0.3059	13.13	1.00	0.52
325	1	Vane	Round	25	0.02	0.02	0.7095	0.6300	0.1661	36.80	0.26	0.18
325	2	Vane	Round	25	0.02	0.02	0.7095	0.4639	0.3061	27.53	0.66	0.25
325	3	Vane	Round	25	0.02	0.02	0.7095	0.1579	0.1359	20.37	0.86	0.33
325	4	Vane	Round	25	0.02	0.02	0.7095	0.0219	0.0219	5.73	1.00	1.00
328	1	Vane	Round	25	0.02	0.02	1.0565	0.9087	0.2232	38.63	0.25	0.18
328	2	Vane	Round	25	0.02	0.02	1.0565	0.6859	0.4024	30.77	0.59	0.22
328	3	Vane	Round	25	0.02	0.02	1.0565	0.2835	0.2019	26.37	0.71	0.26
328	4	Vane	Round	25	0.02	0.02	1.0565	0.0825	0.0825	8.30	1.00	0.82
331	1	Vane	Round	25	0.02	0.02	1.5944	1.4570	0.3350	42.20	0.23	0.16
331	2	Vane	Round	25	0.02	0.02	1.5944	1.1220	0.5567	35.90	0.50	0.19
331	3	Vane	Round	25	0.02	0.02	1.5944	0.5653	0.3030	29.50	0.54	0.23
331	4	Vane	Round	25	0.02	0.02	1.5944	0.2623	0.2623	11.27	1.00	0.60
334	1	bar	Round	25	0.02	0.02	0.6486	0.5885	0.1218	36.53	0.21	0.19
334	2	bar	Round	25	0.02	0.02	0.6486	0.4664	0.3196	31.43	0.69	0.22
334	3	bar	Round	25	0.02	0.02	0.6486	0.1469	0.1231	23.13	0.84	0.29
334	4	bar	Round	25	0.02	0.02	0.6486	0.0239	0.0239	5.77	1.00	1.00
337	1	bar	Round	25	0.02	0.02	1.0106	0.8795	0.1769	40.40	0.20	0.17
337	2	bar	Round	25	0.02	0.02	1.0106	0.7026	0.4100	34.57	0.58	0.20
337	3	bar	Round	25	0.02	0.02	1.0106	0.2926	0.1895	28.10	0.65	0.24

337	4	bar	Round	25	0.02	0.02	1.0106	0.1032	0.1032	10.87	1.00	0.62
340	1	bar	Round	25	0.02	0.02	1.5839	1.4132	0.2845	46.37	0.20	0.15
340	2	bar	Round	25	0.02	0.02	1.5839	1.1285	0.5716	39.10	0.51	0.17
340	3	bar	Round	25	0.02	0.02	1.5839	0.5562	0.2725	30.30	0.49	0.22
340	4	bar	Round	25	0.02	0.02	1.5839	0.2850	0.2850	14.10	1.00	0.48
343	1	Vane	Sq.	25	0.02	0.02	0.6689	0.5410	0.1571	33.73	0.29	0.20
343	2	Vane	Sq.	25	0.02	0.02	0.6689	0.3836	0.2441	26.97	0.64	0.25
343	3	Vane	Sq.	25	0.02	0.02	0.6689	0.1402	0.1354	19.73	0.97	0.34
343	4	Vane	Sq.	25	0.02	0.02	0.6689	0.0048	0.0048	3.93	1.00	1.00
346	1	Vane	Sq.	25	0.02	0.02	1.0094	0.7944	0.2497	37.17	0.31	0.18
346	2	Vane	Sq.	25	0.02	0.02	1.0094	0.5542	0.2821	31.13	0.51	0.22
346	3	Vane	Sq.	25	0.02	0.02	1.0094	0.2659	0.2372	24.43	0.89	0.28
346	4	Vane	Sq.	25	0.02	0.02	1.0094	0.0289	0.0289	8.17	1.00	0.83
349	1	Vane	Sq.	25	0.02	0.02	1.5378	1.3900	0.3815	41.60	0.27	0.16
349	2	Vane	Sq.	25	0.02	0.02	1.5378	1.0130	0.5143	34.73	0.51	0.20
349	3	Vane	Sq.	25	0.02	0.02	1.5378	0.4962	0.3276	30.40	0.66	0.22
349	4	Vane	Sq.	25	0.02	0.02	1.5378	0.1685	0.1685	11.60	1.00	0.58
352	1	bar	Sq.	25	0.02	0.02	0.6830	0.6278	0.1442	35.57	0.23	0.19
352	2	bar	Sq.	25	0.02	0.02	0.6830	0.4836	0.3032	30.70	0.63	0.22
352	3	bar	Sq.	25	0.02	0.02	0.6830	0.1805	0.1704	23.33	0.94	0.29
352	4	bar	Sq.	25	0.02	0.02	0.6830	0.0101	0.0101	4.97	1.00	1.00
355	1	bar	Sq.	25	0.02	0.02	1.0233	0.9229	0.2080	40.20	0.23	0.17
355	2	bar	Sq.	25	0.02	0.02	1.0233	0.7149	0.3706	35.17	0.52	0.19
355	3	bar	Sq.	25	0.02	0.02	1.0233	0.3442	0.2581	28.43	0.75	0.24
355	4	bar	Sq.	25	0.02	0.02	1.0233	0.0862	0.0862	10.40	1.00	0.65
358	1	bar	Sq.	25	0.02	0.02	1.6827	1.4864	0.3446	42.97	0.23	0.16
358	2	bar	Sq.	25	0.02	0.02	1.6827	1.1410	0.5198	37.33	0.46	0.18
358	3	bar	Sq.	25	0.02	0.02	1.6827	0.6225	0.3693	32.03	0.59	0.21
358	4	bar	Sq.	25	0.02	0.02	1.6827	0.2514	0.2514	11.80	1.00	0.57
361	1	Vane	Round	20	0.06	0.02	0.6930	0.6469	0.5210	17.47	0.81	0.39
361	2	Vane	Round	20	0.06	0.02	0.6930	0.1259	0.1259	11.10	1.00	0.61
364	1	Vane	Round	20	0.06	0.02	1.0067	0.9355	0.6385	18.30	0.68	0.37
364	2	Vane	Round	20	0.06	0.02	1.0067	0.2972	0.2972	11.73	1.00	0.58
367	1	Vane	Round	20	0.06	0.02	1.6397	1.4335	0.6308	20.07	0.44	0.34
367	2	Vane	Round	20	0.06	0.02	1.6397	0.8021	0.6686	14.70	0.83	0.46
367	3	Vane	Round	20	0.06	0.02	1.6397	0.1338	0.1338	7.63	1.00	0.89
370	1	bar	Round	20	0.06	0.02	0.6785	0.6422	0.4958	16.40	0.77	0.41
370	2	bar	Round	20	0.06	0.02	0.6785	0.1461	0.1461	7.87	1.00	0.86
373	1	bar	Round	20	0.06	0.02	1.0549	0.9356	0.6900	17.73	0.74	0.38
373	2	bar	Round	20	0.06	0.02	1.0549	0.2457	0.2457	9.93	1.00	0.68
376	1	bar	Round	20	0.06	0.02	1.5635	1.4446	0.9132	20.10	0.63	0.34
376	2	bar	Round	20	0.06	0.02	1.5635	0.5313	0.5246	12.53	0.99	0.54
376	3	bar	Round	20	0.06	0.02	1.5635	0.0068	0.0068	3.47	1.00	1.00
379	1	Vane	Sq.	20	0.06	0.02	0.6759	0.6030	0.5356	13.30	0.89	0.51
379	2	Vane	Sq.	20	0.06	0.02	0.6759	0.0674	0.0674	5.53	1.00	1.00
382	1	Vane	Sq.	20	0.06	0.02	1.0121	0.9165	0.7421	15.27	0.81	0.44
382	2	Vane	Sq.	20	0.06	0.02	1.0121	0.1743	0.1743	6.27	1.00	1.00
385	1	Vane	Sq.	20	0.06	0.02	1.5801	1.4478	0.7854	18.83	0.54	0.36
385	2	Vane	Sq.	20	0.06	0.02	1.5801	0.6624	0.6461	11.40	0.98	0.59
385	3	Vane	Sq.	20	0.06	0.02	1.5801	0.0164	0.0164	3.17	1.00	1.00
388	1	bar	Sq.	20	0.06	0.02	0.6658	0.6143	0.5571	14.90	0.91	0.46
388	2	bar	Sq.	20	0.06	0.02	0.6658	0.0574	0.0574	5.20	1.00	1.00
391	1	bar	Sq.	20	0.06	0.02	1.0737	0.9216	0.7610	17.03	0.83	0.40
391	2	bar	Sq.	20	0.06	0.02	1.0737	0.1605	0.1605	6.90	1.00	0.98
394	1	bar	Sq.	20	0.06	0.02	1.5693	1.4660	1.0230	19.77	0.70	0.34
394	2	bar	Sq.	20	0.06	0.02	1.5693	0.4428	0.4428	10.87	1.00	0.62
397	1	Vane	Round	25	0.06	0.02	0.6908	0.6303	0.5596	14.77	0.89	0.46
397	2	Vane	Round	25	0.06	0.02	0.6908	0.0707	0.0707	6.53	1.00	1.00
400	1	Vane	Round	25	0.06	0.02	1.0985	0.9521	0.7682	16.70	0.81	0.41
400	2	Vane	Round	25	0.06	0.02	1.0985	0.1839	0.1839	7.30	1.00	0.93
403	1	Vane	Round	25	0.06	0.02	1.6475	1.4864	0.9677	19.60	0.65	0.35
403	2	Vane	Round	25	0.06	0.02	1.6475	0.5186	0.5186	11.37	1.00	0.60
406	1	bar	Round	25	0.06	0.02	0.6579	0.5928	0.5099	16.07	0.86	0.42
406	2	bar	Round	25	0.06	0.02	0.6579	0.0829	0.0829	5.67	1.00	1.00
409	1	bar	Round	25	0.06	0.02	0.9630	0.8958	0.7103	17.20	0.79	0.39
409	2	bar	Round	25	0.06	0.02	0.9630	0.1856	0.1856	7.70	1.00	0.88
412	1	bar	Round	25	0.06	0.02	1.6588	1.4723	1.0845	19.27	0.74	0.35
412	2	bar	Round	25	0.06	0.02	1.6588	0.3878	0.3878	10.27	1.00	0.66
415	1	Vane	Sq.	25	0.06	0.02	0.6633	0.6218	0.5369	13.90	0.86	0.49
415	2	Vane	Sq.	25	0.06	0.02	0.6633	0.0849	0.0849	5.20	1.00	1.00
418	1	Vane	Sq.	25	0.06	0.02	0.9996	0.8967	0.7181	16.47	0.80	0.41
418	2	Vane	Sq.	25	0.06	0.02	0.9996	0.1787	0.1787	6.03	1.00	1.00
421	1	Vane	Sq.	25	0.06	0.02	1.6441	1.4490	1.0757	17.47	0.74	0.39
421	2	Vane	Sq.	25	0.06	0.02	1.6441	0.3733	0.3733	8.50	1.00	0.80
424	1	bar	Sq.	25	0.06	0.02	0.6783	0.6215	0.5095	12.40	0.82	0.55

424	2	bar	Sq.	25	0.06	0.02	0.6783	0.1122	0.1122	5.00	1.00	1.00
427	1	bar	Sq.	25	0.06	0.02	1.0407	0.9187	0.6883	15.97	0.75	0.42
427	2	bar	Sq.	25	0.06	0.02	1.0407	0.2304	0.2304	7.47	1.00	0.91
430	1	bar	Sq.	25	0.06	0.02	1.6075	1.4484	1.0278	17.87	0.71	0.38
430	2	bar	Sq.	25	0.06	0.02	1.6075	0.4205	0.4205	9.73	1.00	0.70
433	1	Vane	Round	20	0.02	0.04	0.6533	0.5826	0.4068	27.50	0.70	0.25
433	2	Vane	Round	20	0.02	0.04	0.6533	0.1757	0.1640	18.20	0.93	0.37
433	3	Vane	Round	20	0.02	0.04	0.6533	0.0116	0.0116	6.60	1.00	1.00
436	1	Vane	Round	20	0.02	0.04	1.0458	0.9216	0.5745	28.30	0.62	0.24
436	2	Vane	Round	20	0.02	0.04	1.0458	0.3470	0.2324	20.57	0.67	0.33
436	3	Vane	Round	20	0.02	0.04	1.0458	0.1147	0.1147	13.47	1.00	0.50
439	1	Vane	Round	20	0.02	0.04	1.5837	1.4548	0.5827	32.27	0.40	0.21
439	2	Vane	Round	20	0.02	0.04	1.5837	0.8724	0.4465	26.23	0.51	0.26
439	3	Vane	Round	20	0.02	0.04	1.5837	0.4259	0.3838	20.33	0.90	0.33
439	4	Vane	Round	20	0.02	0.04	1.5837	0.0421	0.0421	7.63	1.00	0.89
442	1	bar	Round	20	0.02	0.04	0.6795	0.6390	0.4222	26.30	0.66	0.26
442	2	bar	Round	20	0.02	0.04	0.6795	0.2168	0.1800	18.43	0.83	0.37
442	3	bar	Round	20	0.02	0.04	0.6795	0.0368	0.0368	7.77	1.00	0.87
445	1	bar	Round	20	0.02	0.04	1.0462	0.9265	0.5166	30.37	0.56	0.22
445	2	bar	Round	20	0.02	0.04	1.0462	0.4099	0.2263	21.63	0.55	0.31
445	3	bar	Round	20	0.02	0.04	1.0462	0.1836	0.1836	11.60	1.00	0.58
448	1	bar	Round	20	0.02	0.04	1.6383	1.4368	0.7198	32.87	0.50	0.21
448	2	bar	Round	20	0.02	0.04	1.6383	0.7171	0.3423	25.07	0.48	0.27
448	3	bar	Round	20	0.02	0.04	1.6383	0.3748	0.3085	21.90	0.82	0.31
448	4	bar	Round	20	0.02	0.04	1.6383	0.0663	0.0663	8.13	1.00	0.83
451	1	Vane	Sq.	20	0.02	0.04	0.6654	0.6128	0.4432	23.33	0.72	0.29
451	2	Vane	Sq.	20	0.02	0.04	0.6654	0.1695	0.1598	15.43	0.94	0.44
451	3	Vane	Sq.	20	0.02	0.04	0.6654	0.0097	0.0097	4.40	1.00	1.00
454	1	Vane	Sq.	20	0.02	0.04	1.0517	0.9201	0.5760	27.97	0.63	0.24
454	2	Vane	Sq.	20	0.02	0.04	1.0517	0.3435	0.2347	19.73	0.68	0.34
454	3	Vane	Sq.	20	0.02	0.04	1.0517	0.1095	0.1095	8.60	1.00	0.79
457	1	Vane	Sq.	20	0.02	0.04	1.5729	1.4406	0.7340	31.03	0.51	0.22
457	2	Vane	Sq.	20	0.02	0.04	1.5729	0.7066	0.3774	24.40	0.53	0.28
457	3	Vane	Sq.	20	0.02	0.04	1.5729	0.3293	0.3141	17.20	0.95	0.39
457	4	Vane	Sq.	20	0.02	0.04	1.5729	0.0152	0.0152	4.87	1.00	1.00
460	1	bar	Sq.	20	0.02	0.04	0.6883	0.6459	0.4140	24.37	0.64	0.28
460	2	bar	Sq.	20	0.02	0.04	0.6883	0.2321	0.1918	16.50	0.83	0.41
460	3	bar	Sq.	20	0.02	0.04	0.6883	0.0404	0.0404	5.70	1.00	1.00
463	1	bar	Sq.	20	0.02	0.04	1.0655	0.9343	0.5364	30.57	0.57	0.22
463	2	bar	Sq.	20	0.02	0.04	1.0655	0.3979	0.2359	20.93	0.59	0.32
463	3	bar	Sq.	20	0.02	0.04	1.0655	0.1621	0.1621	12.97	1.00	0.52
466	1	bar	Sq.	20	0.02	0.04	1.6102	1.4516	0.7240	32.23	0.50	0.21
466	2	bar	Sq.	20	0.02	0.04	1.6102	0.7277	0.3613	25.33	0.50	0.27
466	3	bar	Sq.	20	0.02	0.04	1.6102	0.3665	0.2958	19.90	0.81	0.34
466	4	bar	Sq.	20	0.02	0.04	1.6102	0.0706	0.0706	8.10	1.00	0.84
469	1	Vane	Round	25	0.02	0.04	0.6509	0.6023	0.4271	22.83	0.71	0.30
469	2	Vane	Round	25	0.02	0.04	0.6509	0.1764	0.1476	17.83	0.84	0.38
469	3	Vane	Round	25	0.02	0.04	0.6509	0.0278	0.0278	5.37	1.00	1.00
472	1	Vane	Round	25	0.02	0.04	0.9832	0.9513	0.5850	26.03	0.61	0.26
472	2	Vane	Round	25	0.02	0.04	0.9832	0.3654	0.2468	19.80	0.68	0.34
472	3	Vane	Round	25	0.02	0.04	0.9832	0.1189	0.1189	9.53	1.00	0.71
475	1	Vane	Round	25	0.02	0.04	1.5682	1.4400	0.7819	31.27	0.54	0.22
475	2	Vane	Round	25	0.02	0.04	1.5682	0.6581	0.3515	22.77	0.53	0.30
475	3	Vane	Round	25	0.02	0.04	1.5682	0.3066	0.2837	16.40	0.93	0.41
475	4	Vane	Round	25	0.02	0.04	1.5682	0.0229	0.0229	5.07	1.00	1.00
478	1	bar	Round	25	0.02	0.04	0.6663	0.6210	0.4203	22.47	0.68	0.30
478	2	bar	Round	25	0.02	0.04	0.6663	0.2007	0.1686	16.17	0.84	0.42
478	3	bar	Round	25	0.02	0.04	0.6663	0.0321	0.0321	5.30	1.00	1.00
481	1	bar	Round	25	0.02	0.04	1.0269	0.9375	0.5444	25.93	0.58	0.26
481	2	bar	Round	25	0.02	0.04	1.0269	0.3927	0.2370	22.13	0.60	0.31
481	3	bar	Round	25	0.02	0.04	1.0269	0.1559	0.1559	11.87	1.00	0.57
484	1	bar	Round	25	0.02	0.04	1.5551	1.4255	0.7288	30.87	0.51	0.22
484	2	bar	Round	25	0.02	0.04	1.5551	0.6967	0.3472	24.53	0.50	0.28
484	3	bar	Round	25	0.02	0.04	1.5551	0.3494	0.2795	14.63	0.80	0.46
484	4	bar	Round	25	0.02	0.04	1.5551	0.0699	0.0699	4.50	1.00	1.00
487	1	Vane	Sq.	25	0.02	0.04	0.6547	0.5869	0.4216	22.07	0.72	0.31
487	2	Vane	Sq.	25	0.02	0.04	0.6547	0.1653	0.1579	15.60	0.96	0.43
487	3	Vane	Sq.	25	0.02	0.04	0.6547	0.0073	0.0073	2.73	1.00	1.00
490	1	Vane	Sq.	25	0.02	0.04	1.0131	0.9017	0.5572	24.87	0.62	0.27
490	2	Vane	Sq.	25	0.02	0.04	1.0131	0.3445	0.2488	18.43	0.72	0.37
490	3	Vane	Sq.	25	0.02	0.04	1.0131	0.0957	0.0957	6.20	1.00	1.00
493	1	Vane	Sq.	25	0.02	0.04	1.5687	1.4285	0.7796	30.43	0.55	0.22
493	2	Vane	Sq.	25	0.02	0.04	1.5687	0.6489	0.3522	23.63	0.54	0.29
493	3	Vane	Sq.	25	0.02	0.04	1.5687	0.2967	0.2712	10.20	0.91	0.66
493	4	Vane	Sq.	25	0.02	0.04	1.5687	0.0255	0.0255	3.63	1.00	1.00

496	1	bar	Sq.	25	0.02	0.04	0.6511	0.5928	0.4143	23.20	0.70	0.29
496	2	bar	Sq.	25	0.02	0.04	0.6511	0.1778	0.1581	16.20	0.89	0.42
496	3	bar	Sq.	25	0.02	0.04	0.6511	0.0198	0.0198	2.13	1.00	1.00
499	1	bar	Sq.	25	0.02	0.04	1.0500	0.9381	0.5554	28.23	0.59	0.24
499	2	bar	Sq.	25	0.02	0.04	1.0500	0.3824	0.2471	20.50	0.65	0.33
499	3	bar	Sq.	25	0.02	0.04	1.0500	0.1359	0.1359	9.77	1.00	0.69
502	1	bar	Sq.	25	0.02	0.04	1.5826	1.4527	0.7389	30.90	0.51	0.22
502	2	bar	Sq.	25	0.02	0.04	1.5826	0.7140	0.3721	22.83	0.52	0.30
502	3	bar	Sq.	25	0.02	0.04	1.5826	0.3421	0.2820	15.07	0.82	0.45
502	4	bar	Sq.	25	0.02	0.04	1.5826	0.0599	0.0599	5.50	1.00	1.00
505	1	Vane	Round	20	0.06	0.04	0.6935	0.6810	0.6114	15.50	0.90	0.44
505	2	Vane	Round	20	0.06	0.04	0.6935	0.0697	0.0697	4.97	1.00	1.00
508	1	Vane	Round	20	0.06	0.04	1.0578	0.9099	0.6254	15.87	0.69	0.43
508	2	Vane	Round	20	0.06	0.04	1.0578	0.2851	0.2851	8.67	1.00	0.78
511	1	Vane	Round	20	0.06	0.04	1.5897	1.4565	0.6247	18.23	0.43	0.37
511	2	Vane	Round	20	0.06	0.04	1.5897	0.8317	0.5528	13.13	0.66	0.52
511	3	Vane	Round	20	0.06	0.04	1.5897	0.2791	0.2791	7.37	1.00	0.92
514	1	bar	Round	20	0.06	0.04	0.6702	0.6347	0.6152	14.00	0.97	0.48
514	2	bar	Round	20	0.06	0.04	0.6702	0.0195	0.0195	4.60	1.00	1.00
517	1	bar	Round	20	0.06	0.04	1.0679	0.9123	0.7047	15.97	0.77	0.42
517	2	bar	Round	20	0.06	0.04	1.0679	0.2080	0.2080	6.57	1.00	1.00
520	1	bar	Round	20	0.06	0.04	1.6171	1.4637	0.8518	18.43	0.58	0.37
520	2	bar	Round	20	0.06	0.04	1.6171	0.6092	0.5442	12.00	0.89	0.57
520	3	bar	Round	20	0.06	0.04	1.6171	0.0680	0.0680	4.53	1.00	1.00
523	1	Vane	Sq.	20	0.06	0.04	0.6803	0.6275	0.6150	13.00	0.98	0.52
523	2	Vane	Sq.	20	0.06	0.04	0.6803	0.0126	0.0126	3.83	1.00	1.00
526	1	Vane	Sq.	20	0.06	0.04	1.0321	0.9027	0.7668	15.63	0.85	0.43
526	2	Vane	Sq.	20	0.06	0.04	1.0321	0.1360	0.1360	6.07	1.00	1.00
529	1	Vane	Sq.	20	0.06	0.04	1.5693	1.4436	0.7800	17.47	0.54	0.39
529	2	Vane	Sq.	20	0.06	0.04	1.5693	0.6639	0.6204	10.53	0.93	0.64
529	3	Vane	Sq.	20	0.06	0.04	1.5693	0.0436	0.0436	3.27	1.00	1.00
532	1	bar	Sq.	20	0.06	0.04	0.6720	0.6288	0.6079	13.40	0.97	0.51
532	2	bar	Sq.	20	0.06	0.04	0.6720	0.0208	0.0208	3.97	1.00	1.00
535	1	bar	Sq.	20	0.06	0.04	1.0309	0.8737	0.7751	15.70	0.89	0.43
535	2	bar	Sq.	20	0.06	0.04	1.0309	0.0985	0.0985	5.63	1.00	1.00
538	1	bar	Sq.	20	0.06	0.04	1.6362	1.4440	0.9321	18.03	0.65	0.38
538	2	bar	Sq.	20	0.06	0.04	1.6362	0.5120	0.4748	10.80	0.93	0.63
538	3	bar	Sq.	20	0.06	0.04	1.6362	0.0373	0.0373	3.37	1.00	1.00
541	1	Vane	Round	25	0.06	0.04	0.6753	0.6391	0.6229	12.67	0.97	0.54
541	2	Vane	Round	25	0.06	0.04	0.6753	0.0164	0.0164	3.13	1.00	1.00
544	1	Vane	Round	25	0.06	0.04	1.0485	0.9193	0.8425	15.00	0.92	0.45
544	2	Vane	Round	25	0.06	0.04	1.0485	0.0769	0.0769	4.40	1.00	1.00
547	1	Vane	Round	25	0.06	0.04	1.6442	1.4570	0.9295	17.83	0.64	0.38
547	2	Vane	Round	25	0.06	0.04	1.6442	0.5274	0.5274	10.57	1.00	0.64
550	1	bar	Round	25	0.06	0.04	0.6471	0.6187	0.6152	14.03	0.99	0.48
550	2	bar	Round	25	0.06	0.04	0.6471	0.0036	0.0036	2.40	1.00	1.00
553	1	bar	Round	25	0.06	0.04	1.0473	0.9222	0.8280	15.80	0.90	0.43
553	2	bar	Round	25	0.06	0.04	1.0473	0.0942	0.0942	4.67	1.00	1.00
556	1	bar	Round	25	0.06	0.04	1.6377	1.4431	1.1481	18.30	0.80	0.37
556	2	bar	Round	25	0.06	0.04	1.6377	0.2952	0.2952	8.43	1.00	0.80
559	1	Vane	Sq.	25	0.06	0.04	0.6757	0.6290	0.6075	13.67	0.97	0.50
559	2	Vane	Sq.	25	0.06	0.04	0.6757	0.0214	0.0214	2.73	1.00	1.00
562	1	Vane	Sq.	25	0.06	0.04	1.0394	0.9091	0.8208	15.23	0.90	0.45
562	2	Vane	Sq.	25	0.06	0.04	1.0394	0.0884	0.0884	4.50	1.00	1.00
565	1	Vane	Sq.	25	0.06	0.04	1.5741	1.4334	1.1492	17.70	0.80	0.38
565	2	Vane	Sq.	25	0.06	0.04	1.5741	0.2843	0.2843	7.40	1.00	0.92
568	1	bar	Sq.	25	0.06	0.04	0.6508	0.6167	0.6058	13.23	0.98	0.51
568	2	bar	Sq.	25	0.06	0.04	0.6508	0.0110	0.0110	3.03	1.00	1.00
571	1	bar	Sq.	25	0.06	0.04	1.0233	0.8776	0.7772	15.10	0.89	0.45
571	2	bar	Sq.	25	0.06	0.04	1.0233	0.1004	0.1004	4.10	1.00	1.00
574	1	bar	Sq.	25	0.06	0.04	1.5915	1.4382	1.1312	17.87	0.79	0.38
574	2	bar	Sq.	25	0.06	0.04	1.5915	0.3070	0.3070	8.43	1.00	0.80

Appendix F: Experimental Data for Grate Erosion Rate Test

LEGEND

TU = upstream spread measurement (cm)

TD = downstream spread measurement (cm)

wb = weight before test of clogging material (g)

ws = Weight after experiment fully saturated (g)

wd = weight after experiment fully dry (g)

Table 14. Experimental data for sediment removal test.

Starting Trial	Grate	Cross Slope	Long Slope	Inflow (m^3/hr.)	TU (cm)	TD (cm)	wb (g)	ws (g)	wd (g)	Time (s)
1	bar	0.06	0.04	0.68	7.5	3.7	26.4	16.0	20.0	614
4	bar	0.06	0.04	1.04	10.0	5.0	28.4	13.1	15.1	405
7	bar	0.06	0.04	1.45	13.2	7.7	32.1	8.3	6.5	318
10	vane	0.06	0.04	0.68	8.8	1.0	30.2	12.7	10.7	500
13	vane	0.06	0.04	1.09	11.5	4.7	38.3	0.3	1.2	187
16	vane	0.06	0.04	1.32	13.9	8.1	36.5	5.5	3.0	342
19	bar	0.02	0.04	0.77	15.1	7.1	33.3	24.5	22.1	530
22	bar	0.02	0.04	1.04	18.6	10.7	34.0	30.0	26.9	584
25	bar	0.02	0.04	1.54	23.3	16.3	30.8	17.8	14.9	436
28	vane	0.02	0.04	0.75	19.3	13.0	31.2	24.1	18.7	540
31	vane	0.02	0.04	1.07	22.6	14.6	31.9	17.9	14.7	412
34	vane	0.02	0.04	1.59	28.8	19.4	32.9	20.9	17.7	640
37	bar	0.06	0.02	0.70	14.8	9.1	35.0	30.2	27.9	667
40	bar	0.06	0.02	1.07	20.0	10.7	34.6	17.9	14.7	654
43	bar	0.06	0.02	1.59	22.0	14.9	34.5	18.3	14.5	508
46	vane	0.06	0.02	0.70	15.8	10.0	28.1	14.0	11.7	544
49	vane	0.06	0.02	1.09	19.2	10.8	30.3	5.2	3.6	422
52	vane	0.06	0.02	1.59	22.3	12.5	29.7	15.3	12.7	417
55	bar	0.02	0.02	0.68	28.9	23.9	35.9	30.6	26.7	577
58	bar	0.02	0.02	1.04	33.3	31.8	30.9	20.2	17.3	556
61	bar	0.02	0.02	1.57	37.9	34.3	27.7	14.2	8.9	472
64	vane	0.02	0.02	0.70	33.1	31.1	33.2	24.8	20.5	617
67	vane	0.02	0.02	1.02	35.7	34.6	33.5	20.5	17.5	620
70	vane	0.02	0.02	1.61	40.9	40.0	28.5	8.5	7.1	426
73	bar	0.06	0.01	0.70	19.6	13.9	32.0	23.6	19.5	586
76	bar	0.06	0.01	1.07	23.7	17.5	35.6	12.7	10.2	544
79	bar	0.06	0.01	1.66	29.7	27.0	30.1	13.9	11.2	554

82	vane	0.06	0.01	0.70	18.4	15.0	32.7	19.3	15.4	496
85	vane	0.06	0.01	1.04	22.4	18.5	35.3	17.5	14.5	573
88	vane	0.06	0.01	1.64	29.2	21.3	31.9	20.6	16.4	585
91	bar	0.02	0.01	0.73	35.9	32.1	33.9	29.2	24.3	582
94	bar	0.02	0.01	1.09	39.2	36.9	29.5	28.8	22.1	583
97	bar	0.02	0.01	1.64	44.9	43.2	30.4	15.1	11.7	540
100	vane	0.02	0.01	0.66	35.3	25.0	33.7	25.7	21.6	582
103	vane	0.02	0.01	1.02	39.1	33.7	27.8	19.3	16.8	518
106	vane	0.02	0.01	1.61	44.7	44.8	29.5	19.2	15.8	569
109	bar	0.06	0.005	0.73	22.1	16.6	33.5	28.0	24.3	614
112	bar	0.06	0.005	1.07	25.9	20.2	28.5	19.0	16.0	536
115	bar	0.06	0.005	1.68	30.5	25.5	30.6	20.6	17.9	597
118	vane	0.06	0.005	0.73	23.0	18.0	27.9	20.0	17.4	684
121	vane	0.06	0.005	1.07	27.1	20.9	24.9	14.4	12.4	561
124	vane	0.06	0.005	1.61	30.5	23.2	27.5	17.7	14.9	610
127	bar	0.02	0.005	0.70	46.3	47.5	25.9	11.7	9.6	585
130	bar	0.02	0.005	1.09	49.1	52.2	30.7	16.6	13.0	473
133	bar	0.02	0.005	1.61	52.6	51.5	29.7	6.8	5.4	550
136	vane	0.02	0.005	0.68	43.8	41.7	27.4	16.4	15.9	568
139	vane	0.02	0.005	1.04	50.8	48.6	30.7	22.1	14.0	460
142	vane	0.02	0.005	1.59	57.3	51.9	35.6	0.0	0.0	474

Appendix G: Design Details

The following were detail drawings provided by Kansas and Illinois DOTs used for 3D prints.

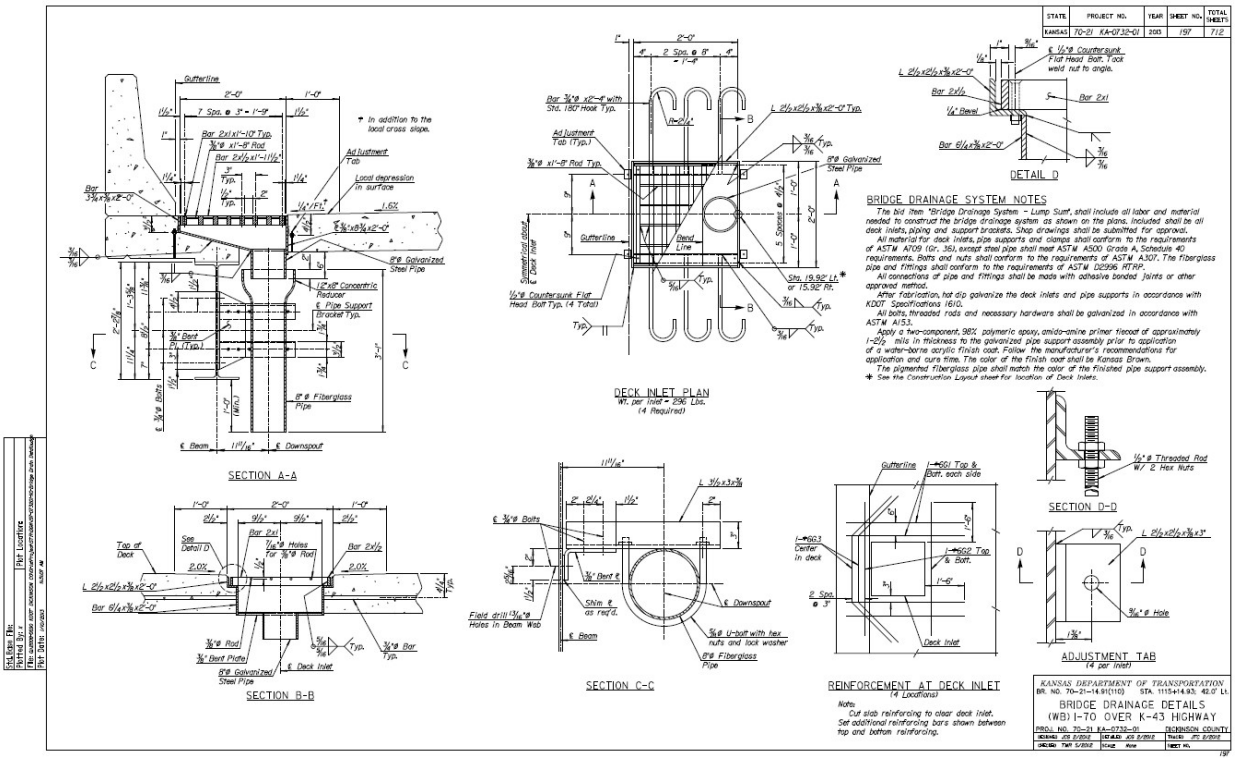

Figure 15. Standard 0.61-m x 0.61-m drainage detail with bar grate from the Kansas Department of Transportation Bridge Design Manual (2016).

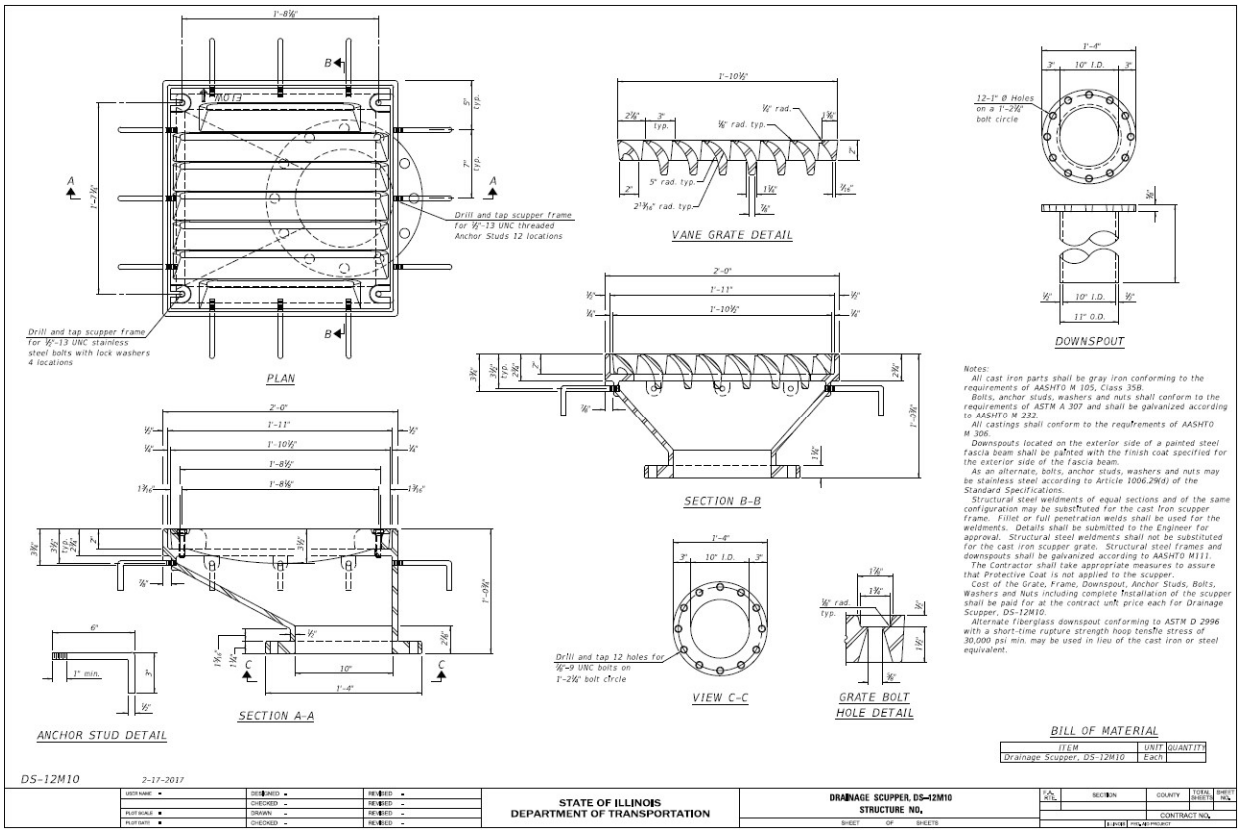

Figure 16. Illinois curve vane grate design provided by ILDOT engineer.